Paleoceanography and Paleoclimatology

RESEARCH ARTICLE
10.1029/2021PA004241

Early Paleocene Paleoceanography and Export Productivity in the Chicxulub Crater

Christopher M. Lowery[1], Heather L. Jones[2,3], Timothy J. Bralower[2], Ligia Perez Cruz[4], Catalina Gebhardt[5], Michael T. Whalen[6], Elise Chenot[7,8], Jan Smit[9], Marcie Purkey Phillips[1], Konstantin Choumiline[10], Ignacio Arenillas[11], Jose A. Arz[11], Fabien Garcia[12], Myriam Ferrand[12], Sean P. S. Gulick[1,13,14], and Expedition 364 Science Party

[1]Institute for Geophysics, Jackson School of Geosciences, University of Texas at Austin, Austin, TX, USA, [2]Department of Geosciences, Pennsylvania State University, University Park, PA, USA, [3]MARUM-Center for Marine Environmental Sciences, University of Bremen, Bremen, Germany, [4]Instituto de Geofísica, Universidad Nacional Autónoma De México, Ciudad de México, México, [5]Alfred Wegener Institute Helmholtz Centre of Polar and Marine Research, Bremerhaven, Germany, [6]Department of Geosciences, University of Alaska Fairbanks, Fairbanks, AK, USA, [7]Géosciences Montpellier, Université de Montpellier, Montpellier, France, [8]Institut Polytechnique Lasalle Beauvais, Beauvais, France, [9]Faculty of Earth and Life Sciences (FALW), Vrije Universiteit Amsterdam, Amsterdam, The Netherlands, [10]Department of Earth Sciences, University of California Riverside, Riverside, CA, USA, [11]Departamento de Ciencias de la Tierra and Instituto Universitario de Investigación en Ciencias Ambientales de Aragón, Universidad de Zaragoza, Zaragoza, Spain, [12]Biogéosciences, Université de Bourgogne Franche-Comté, Dijon, France, [13]Department of Geological Sciences, Jackson School of Geosciences, University of Texas at Austin, Austin, TX, USA, [14]Center for Planetary Systems Habitability, Jackson School of Geosciences, University of Texas at Austin, Austin, TX, USA

Abstract The Chicxulub impact caused a crash in productivity in the world's oceans which contributed to the extinction of ~75% of marine species. In the immediate aftermath of the extinction, export productivity was locally highly variable, with some sites, including the Chicxulub crater, recording elevated export production. The long-term transition back to more stable export productivity regimes has been poorly documented. Here, we present elemental abundances, foraminifer and calcareous nannoplankton assemblage counts, total organic carbon, and bulk carbonate carbon isotope data from the Chicxulub crater to reconstruct changes in export productivity during the first 3 Myr of the Paleocene. We show that export production was elevated for the first 320 kyr of the Paleocene, declined from 320 kyr to 1.2 Myr, and then remained low thereafter. A key interval in this long decline occurred 900 kyr to 1.2 Myr post impact, as calcareous nannoplankton assemblages began to diversify. This interval is associated with fluctuations in water column stratification and terrigenous flux, but these variables are uncorrelated to export productivity. Instead, we postulate that the turnover in the phytoplankton community from a post-extinction assemblage dominated by picoplankton (which promoted nutrient recycling in the euphotic zone) to a Paleocene pelagic community dominated by relatively larger primary producers like calcareous nannoplankton (which more efficiently removed nutrients from surface waters, leading to oligotrophy) is responsible for the decline in export production in the southern Gulf of Mexico.

Plain Language Summary The end Cretaceous mass extinction was caused by the impact of an asteroid in what is now the Yucatán Peninsula, México. The impact ejected aerosols and dust into the air that reduced sunlight transmission, causing a severe decline in photosynthesis and the collapse of marine food webs. However, the change in the amount of organic matter created by photosynthesizing plankton that was delivered to the seafloor (export productivity) was variable across the oceans. At some places, including the Chicxulub crater, export productivity was actually high immediately after the impact. We produced a ~3-million -year record of export productivity in the crater to determine how long it remained elevated and why it eventually declined. Export production was very high for the first 320,000 years after the impact, declined from 320,000 to 1,200,000 years after the impact, and then remained low. We found that this production was not related to the input of nutrients nor the degree of stratification of the ocean, but instead was probably driven by the increase in the cell size of phytoplankton. Larger phytoplankton removed nutrients from the surface waters as they sank, prompting an increase in species which are better adapted to low-nutrient waters.

The author and affiliation details of Expedition 364 Science Party are mentioned in the section Appendix A.

Key Points:

- Export productivity at Chicxulub was elevated for 1.2 Myr post K-Pg; it was very high for the first 0.32 Myr and declined from 0.32–1.2 Myr
- The final decline in export productivity ~0.9–1.2 Myr is associated with the termination of calcareous nannoplankton disaster assemblages
- Export productivity change is not correlated with stratification or terrigenous input and was likely driven by changes in the phytoplankton

Correspondence to:
C. M. Lowery,
cmlowery@utexas.edu

Citation:
Lowery, C. M., Jones, H. L., Bralower, T. J., Cruz, L. P., Gebhardt, C., Whalen, M. T., et al. (2021). Early Paleocene paleoceanography and export productivity in the Chicxulub crater. *Paleoceanography and Paleoclimatology, 36*, e2021PA004241. https://doi.org/10.1029/2021PA004241

Received 15 FEB 2021
Accepted 27 SEP 2021

1. Introduction

At the end of the Cretaceous Period (66.0 Ma), the impact of an asteroid on the Yucatán carbonate platform in the southern Gulf of Mexico caused the extinction of ~75% of marine species (Alvarez et al., 1980; Hildebrand et al., 1991; Jablonski, 1995; Schulte et al., 2010; Smit & Hertogen, 1980), including ~90% of pelagic calcifiers such as planktic foraminifera and calcareous nannoplankton (Bown et al., 2004; Fraass et al., 2015; Lowery et al., 2020). Dust and sulfate aerosols ejected from the evaporite-rich carbonates of the target rock, soot from wildfires, and petrogenic carbon from the crater (Kaiho et al., 2016; Lyons et al., 2020) blocked the sun, resulting in severe short-term cooling (Artemieva & Morgan, 2020; Artemieva et al., 2017; Bardeen et al., 2017; Brugger et al., 2017; Vellekoop et al., 2014, 2016; Gulick et al., 2019; Pope et al., 1994; Wolbach et al., 1985) and collapse of the food chain due to a sharp decline in photosynthesis (D'Hondt et al., 1998; Kring, 2007; Gibbs et al., 2020; Zachos et al., 1989). These effects were short-lived, however, as most dust, soot, and aerosols were removed from the atmosphere on the order of years (Brugger et al., 2017; Tabor et al., 2020), and the oceans quickly became hospitable for life, even at ground zero in the Chicxulub crater (Lowery et al., 2018). Recent work quantifying oceanic pH changes across the K-Pg boundary has shown that minor (0.25 pH decrease) post-impact upper ocean acidification lasted for ~40 kyr, and pH values returned to pre-event values within 80 kyr, after a period of overshoot (Henehan et al., 2019). Meanwhile, temperature proxies and modeling data indicate that Deccan volcanism in the early Paleocene was insufficient to negatively impact early recovery ecosystems (Hull et al., 2020).

Given the short duration of adverse environmental conditions in the earliest Paleocene, it is puzzling that global marine productivity took at least 1.8 Myr to recover to pre-extinction levels (e.g., Birch et al., 2016, 2021; Coxall et al., 2006; D'Hondt et al., 1998; D'Hondt & Zachos, 1993; Hsü & McKenzie, 1985; Zachos et al., 1989). The reduction of export productivity (the amount of organic matter removed from the surface ocean to the ocean interior) at the K-Pg boundary has been proposed based on changes in the vertical gradient of $\delta^{13}C$ between the surface ocean and seafloor. Under normal conditions, the sinking of ^{12}C-enriched organic carbon (primarily driven by the sinking remains of dead plankton, vertically migrating live plankton, and other biological pathways collectively termed the "biological pump") from the euphotic zone to the deep sea leaves the surface ocean enriched in ^{13}C and the seafloor depleted in ^{13}C (e.g., see Birch et al., 2016). The post-K-Pg collapse in this gradient can be explained by a 50% reduction in the amount of organic matter exported from the euphotic zone (Alegret et al., 2012; D'Hondt et al., 1998; Henehan et al., 2019) or less, if part of the signal is from extinction-related changes in planktic foraminifer shell geochemistry (e.g., the extinction of photosymbiont-bearing planktics; Alegret et al., 2012; Birch et al., 2016) and/or the proportion of non-biogenic carbonate in the fine fraction (e.g., Minoletti et al., 2005). However, the exact mechanisms which controlled the eventual recovery of export productivity, and, vitally, the relationship between the recovery of export production and the recovery of marine ecosystems remain unclear.

Biogenic barium is a paleoproductivity proxy which correlates with local organic matter flux from overlying surface water, or export production (e.g., Paytan & Griffith, 2007) and, unlike the carbon isotope proxy, does not require pristine foraminifera to reconstruct, allowing it to be applied to more sites. XRF-derived "excess" barium proxy data indicate that export production did not uniformly decline across the oceans after the Chicxulub impact, as some sites show an increase (Hull & Norris, 2011). Broadly, sites from a range of water depths in the Gulf of Mexico/North Atlantic/Tethys region record reduced export production in the earliest Danian (Alegret et al., 2001; Vellekoop et al., 2017), whereas sites in the central Pacific record increased export production during the same time period (Hull & Norris, 2011). A new earliest Danian record from the peak ring of the Chicxulub crater at joint International Ocean Discovery Program (IODP) International Continental Drilling Project (ICDP) Site M0077 revealed that the crater itself experienced high export productivity immediately after the impact. This high export productivity lasted at least to planktic foraminifer biozone Pα, a few 10s of kyrs after the impact (Lowery et al., 2018).

A great deal of work in the Chicxulub crater has focused on the immediate aftermath of the impact, including the (re)appearance of planktic foraminifera, calcareous nannoplankton, calcispheres (calcareous dinoflagellate resting cysts), and cyanobacteria below the iridium layer, and thus within a few years of the impact (Bralower et al., 2020a, 2020b; Lowery et al., 2018; Schaefer et al., 2020). Recent modeling work by Brugger et al. (2021) suggests a global burst of net primary production fueled by nutrients from ocean

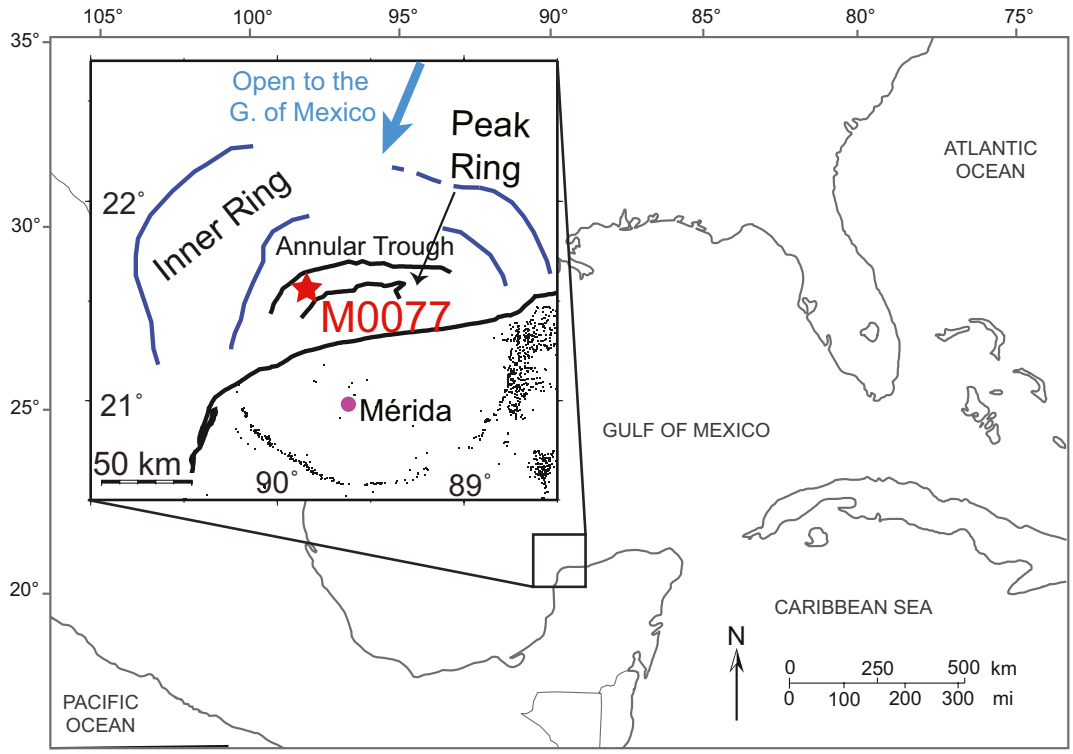

Figure 1. Location map showing the position of International Ocean Discovery Program Site M0077 within the Chicxulub crater.

overturning and dust, beginning a few years after the impact and persisting for as much as a thousand years, which is supported by these observations of early primary producers from the Chicxulub crater.

However, immediate effects of the impact like fallout of dust and a breakdown of ocean stratification are insufficient to explain the longer-term increase in export production observed at some sites like Chicxulub. In fact, it is unclear how long high export productivity persisted at ground zero or how it relates to global patterns of export production in the earliest Danian. Was this locality oceanographically pre-disposed to high export productivity, or did changing local conditions eventually lead to a decline? If so, how did environment or ecology shift to cause lower export production? Jones et al. (2019) found that calcareous nannoplankton "disaster assemblages" persisted in the crater for approximately 1 Myr post impact, well after they were replaced by incoming Paleocene taxa at other sites. Interestingly, the turnover from disaster assemblages to a succession of acmes of novel Paleocene nannoplankton species in the crater is associated with a shift in surface waters from eutrophic to oligotrophic conditions (Jones et al., 2019). Jones et al. (2019) speculated that these changes in the populations of primary producers and surface water nutrients are related to changes in export productivity, but lacked the data to test this hypothesis.

Here, we compare the calcareous nannoplankton record of Jones et al. (2019) to new planktic and benthic foraminifera, major, minor, and trace element data from the early Paleocene interval (66.0–62.5 Ma) at IODP/ICDP Site M0077 in the Chicxulub crater (Figure 1). These data allow us to (a) reconstruct export productivity, water column stratification, terrigenous flux, and phytoplankton population change, (b) document the overall paleoceanographic evolution of the crater and (c) determine how long export production remained elevated after the K-Pg boundary. We then evaluate competing hypotheses about the causes of the eventual decline in export production: environmental changes in the southern Gulf of Mexico or ecological changes in the plankton community.

2. Material and Methods

In 2016, IODP/ICDP Expedition 364 drilled Site M0077 in the peak ring of the Chicxulub crater (Morgan et al., 2017), coring over 100 m of post-impact Paleogene sediments with nearly 100% recovery. Ten meters of Paleocene pelagic carbonates were recovered at the base of the post-impact section, conformably overlying the top of the impact breccia. The uppermost 40 cm of these pelagic carbonates is cut by three disconformities and spans the middle and late Paleocene (Smith et al., 2020); the rest of the section, the focus of this study, spans the earliest to middle Paleocene, from 66 to ~62 Ma (Morgan et al., 2017).

2.1. Microfossils

Samples for foraminiferal analysis were crushed with mortar and pestle into mm-sized pieces and then soaked in a solution of peroxide and borax for at least one week. They were then sieved over a 45 μm mesh to ensure recovery of generally small Paleocene taxa (care was taken to avoid juveniles in the counts, but many mature specimens–i.e., with multiple whorls–smaller than the more common 63 μm cutoff were present). The sieve was soaked in methylene blue dye between samples to identify contamination. Sieved samples were dried in an oven and then split in a microsplitter to obtain a manageable number of foraminifera. At least 300 individuals were picked per sample. Additional specimens were extracted using a solution with 80% acetic acid and 20% H_2O, following the procedure of Lirer (2000). The best-preserved of these were imaged with the Zeiss MERLIN Field Emission Scanning Electron Microscope (FESEM) at the Universidad de Zaragoza.

2.2. XRF Core Scanning

Split cores were scanned with an AVAATECH XRF Core Scanner II at the University of Bremen. The split core surface was covered with a 4-μm thick SPEXCerti Prep Ultralene foil to avoid contamination of the core material. Data were collected with a Canberra X-PIPS Silicon Drift Detector (Model SXD 15C-1150-500) with a 1,550 eV X-ray resolution, the Canberra Digital Spectrum Analyzer DAS 1000, and an Oxford Instruments 50W XTF5011 X-Ray tube with rhodium target material, and ray data were processed using the iterative least squares software WIN AXIL from Canberra Eurisys. To obtain sufficient resolution, we used a slit-size of 12 mm and a step-size of 10 mm. We conducted three line-scans to determine a range of element concentrations across the core section. For the first scan, we used an accelerating voltage of 50 kV and a beam current of 1 mA with a sampling time of 20 s to determine the concentrations of Ba and Sr. For the second scan, we used an accelerating voltage of 30 kV and a beam current of 1 mA with a sampling time of 20 s to determine the concentrations of Sr, Rb, Zr, Zn, Pb, and Ni. For the third scan, we used an accelerating voltage of 10 kV and a beam current of 0.15 mA with a sampling time of 20 s to determine the concentrations of Al, Si, K, Ca, Ti, Fe, Mn, and S. Ba, Ti, Al, Fe, and Ca scans are reported here.

2.3. Total Organic Carbon

Total organic carbon (TOC) was determined by measuring the difference between total carbon (TC) and total inorganic carbon (TIC). TC and TIC were determined via ignition and acidification, respectively, both of which produced CO_2 which was quantified with the infrared analyzer on an ELTRA CS500 carbon sulfur analyzer, with analytical error of <2%.

2.4. Carbon Stable Isotopes

Bulk rock samples were taken every 5 cm for stable isotope analysis at the Biogéosciences Laboratory, University of Bourgogne Franche-Comté, Dijon, France. Samples were crushed in an agate mortar and pestle into fine and homogeneous calcite powders, which were reacted with 100% phosphoric acid at 70°C using a ThermoScientific DELTA V PLUS mass spectrometer, connected to a Kiel IV carbonate preparation device. All isotopic values are reported in the standard δ-notation in per mil relative to VPDB (Vienna Pee Dee Belemnite) by assigning a $\delta^{13}C$ value of +1.95‰ to NBS19. External reproducibility as determined by replicate analyses of laboratory standards was ±0.04‰ (2σ) for carbon isotopes.

Table 1
Biostratigraphic Datums for the Paleocene Interval of Hole M0077A

Event	Taxon	Zone	Sample above	Sample below	Avg. Depth	Datum age
B	*Morozovella aequa*	Base of P4c	607.52	607.76	607.65	57.79
B	*Heliolithus kleinpellii*	Base of CP5	607.52	607.76	607.65	59.54
B	*S. moriformis*	Base of CNP6	607.52	607.76	607.65	62.10
B	*Igorina pusilla*	Base of P3a	609.28	609.30	609.29	62.30
B	*Praemurica uncinata*	Base of P2	610.60	610.65	610.63	62.60
B	*Prinsius martinii*[a]	Base of CNP4	614.02	614.07	614.05	63.66
B	*Globanomalina compressa*	Base of P1c	612.36	612.41	612.39	63.90
B	*Chiasmolithus danicus*[a]	Base of CP2	612.50	612.75	612.63	64.81
B	*Prinsius dimorphosus*[a]	Base of CNP3	613.35	613.40	613.38	65.24
B	*Subbotina triloculinoides*	Base of P1b	615.21	615.26	615.24	65.25
T	*Parvularugoglobigerina eugubina*	Base of P1a	616.15	616.20	616.18	65.72
B	*Cruciplacoluthis intermedius*[a]	CP1b	614.07	614.13	614.10	65.70
B	*Coccolithus pelagicus*[a]	CNP2	616.44	616.45	616.45	65.07
B	*Parvularugoglobigerina eugubina*	Base Pα	616.56	616.56	616.56	66.00

Note. Datum ages after Gradstein et al. (2012). Note that datums are listed in chronologic order and that therefore some are out of stratigraphic order.
[a]These nannofossil datums are not used in the age model.

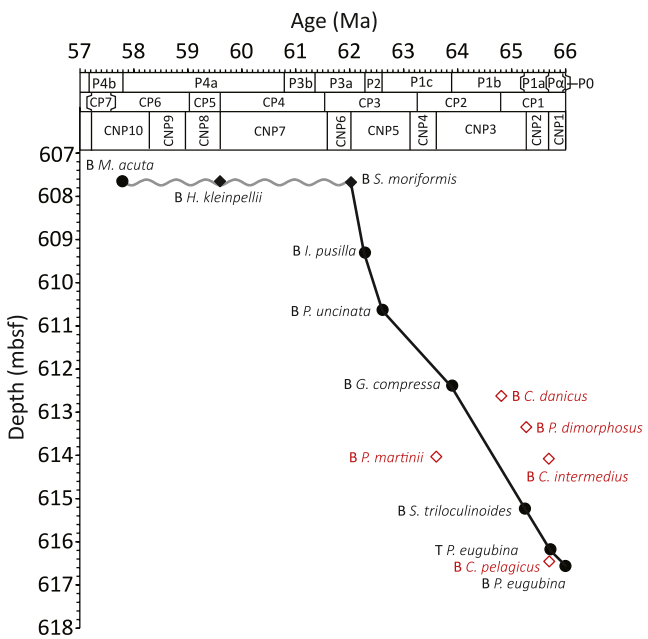

Figure 2. Age-depth plot showing the construction of the age model. Black circles are planktic foraminifer datums, black diamonds are calcareous nannoplankton datums used in the age model, and open diamonds are calcareous nannoplankton datums which appear out of place and are not used in the age model. P zones are planktic foraminifer and CP zones are calcareous nannoplankton. The study focuses on the first ~3.5 Myr of the Paleocene, to the base of planktic foraminifer zone P2.

3. Results

3.1. Age Model

The age model used here (Table 1; Figure 2) represents an update from that published by the Expedition 364 Science Party (Gulick et al., 2017), including small refinements in the placement of biozones and the identification of an unconformity at ~607.8 mbsf (above the interval we discuss here). Calcareous nannofossil biostratigraphy is based on the CP zonation scheme of Okada and Bukry (1980) and the CNP scheme of Agnini et al. (2014), following the taxonomic concepts of Perch-Nielsen (1985) and Bown (1998). Planktic foraminifer biostratigraphy is based on the P zones of Berggren and Pearson (2005) as modified by Wade et al. (2011), following the taxonomic concepts of Olsson et al. (1999) and Pearson et al. (2006). Key planktic foraminifer taxa are illustrated in Figure 3. Calibrated ages assigned to each datum are those reported in Appendix 3 of the Geologic Time Scale 2012 (Gradstein et al., 2012). Samples were taken at 2 cm increments from 616.2–616.6 mbsf, and 5 cm increments above that. Paleomagnetic reversals are not included in the age model because a heterogeneous chemical remnant re-magnetization occurred throughout the study interval obscuring the original polarity (Gulick et al., 2019; Morgan et al., 2017).

Although planktic foraminifera are abundant and diverse throughout the study interval, calcareous nannoplankton are less abundant and a number of key taxa are missing. Nannoplankton zonal markers in the early Paleocene at Site M0077 are either absent (bases of CP3, CP4 and CNP5) or inconsistent with the planktic foraminifer datums (bases of CP1b, CP2, CP5, CNP2-CNP4) (red diamonds on Figure 2). Jones et al. (2019) showed that acmes of several of these markers are globally diachronous. On the other hand, first and last occurrences of biostratigraphically significant planktic foraminifera taxa occur in the correct order and seem to indicate

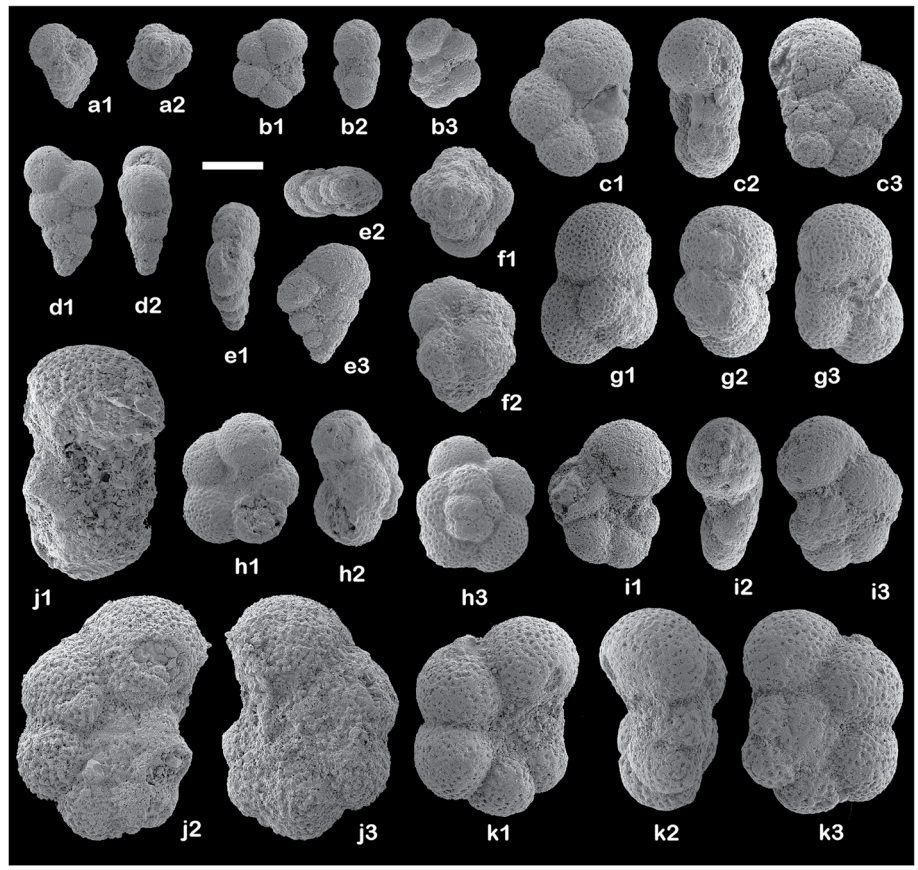

Figure 3. SEM images of planktic foraminiferal index-species and other relevant species (scale bar = 100 microns). (a) *Guembelitria cretacea* (364-M0077A-39R-2 85–86 cm); (b) *Parvularugoglobigerina eugubina* (364-M077A-40R-1 17–18 cm); (c) *Parasubbotina pseudobulloides* (364-M0077A-39R-1 128–129 cm); (d) *Chiloguembelina morsei* (364-M0077A-39R-2 98–99 cm); (e) *Chiloguembelina midwayensis* (364-M0077A-39R-3 41–42 cm); (f) *Globoconusa daubjergensis* (364-M0077A-37R-2 116–117 cm); (g) *Subbotina triloculinoides* (364-M0077A-38R-2 60–61 cm); (h) *Eoglobigerina edita* (364-M077A-38R-2 60–61 cm); (i) *Globanomalina compressa* (364-M0077A-37R-1 116–117 cm); (j) *Praemurica uncinata* (364-M077A-37R-1 96–97 cm); (k) *Praemurica inconstans* (364-M0077A-37R-2 37–38 cm).

relatively constant sedimentation rates over the study interval (from the base of the Paleocene to planktic foraminifer biozone P2). Additionally, planktic foraminifer acme events (e.g., Arenillas et al., 2000) occur within the expected planktic foraminiferal biozones at Site M0077 (see Section 4 below). For these reasons, we consider the nannofossil datums at our site to be unreliable for age control and do not include them in the age model. We are confident the first and last occurrence datums of planktic foraminifera in the Chicxulub crater are coeval with those in the global ocean, and thus we have used planktic foraminifer biozones listed in Table 1 to construct the age model. See Data Availability Statement for links to full foraminifera and calcareous nannoplankton counts.

3.2. M0077 Sedimentology and Terrigenous Flux

The Paleocene interval at Site M0077 is primarily pelagic carbonate with varying degrees of dilution by terrigenous material (Figure 4). Magnetic susceptibility is a common tool to determine the terrigenous component in pelagic carbonates (e.g., Liu et al., 2012), although without determining the source of the magnetic signal it loses some meaning, and so we use elemental data to provide more detail.

Iron is generally correlated with terrigenous flux, while calcium is primarily sourced from biogenic carbonate (Rothwell & Croudace, 2015). Both Fe and Ca are often used to infer carbonate dissolution in deep sea cores, particularly during the Paleogene, which was characterized by discrete episodes of CO_2 release,

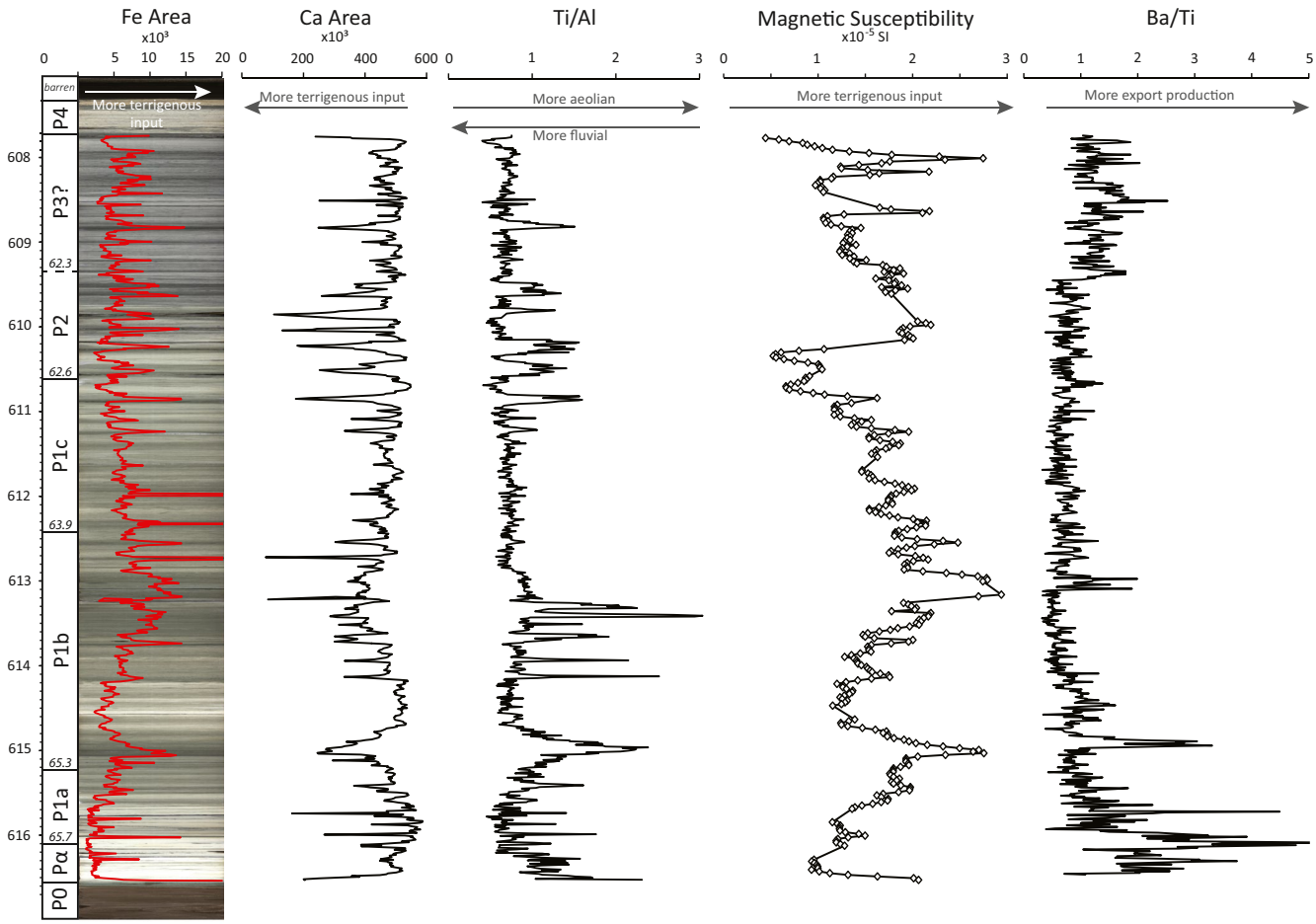

Figure 4. Sedimentological proxies versus depth. Core linescan composite of the Paleocene interval at Site M0077 is overlaid by XRF Fe counts. Increased Fe, decreased Ca, increased Ti/Al, and higher magnetic susceptibility are all proxies for higher terrigenous flux. Increased Ba/Ti indicated higher local export productivity.

warming, and ocean acidification (Bralower et al., 2002; Coccioni et al., 2010; Edgar et al., 2007; Quillévéré et al., 2008). However, we conclude that Fe and Ca variations at Site M0077 were driven by changes in dilution of carbonate by terrigenous material rather than dissolution of carbonate because: (a) The site is relatively shallow (~700 m water depth) in the Paleocene (Lowery et al., 2018), well above the early Paleocene lysocline; and, (b) intervals of elevated Fe/depressed Ca do not correspond to levels of reduced foraminifer preservation (Figure 5). Core material at Site M0077 is strongly lithified, and had to be broken down with a mortar and pestle prior to soaking. An unfortunate side effect of this aggressive disaggregation is the fracturing of some of the foraminiferal tests, which would bias a common proxy for carbonate dissolution, the "Foram Fractionation Index" (Thunell, 1976). In order to establish some quantitative proxy for foraminifer preservation, we instead report the number of individuals in each counted population that could not be identified to the genus level. These "planktic spp." are excluded from population analysis (other than planktic/benthic ratio) but provide a useful approximation of preservation, with more unidentifiable individuals indicating worse preservation. Figure 5 shows the lack of correlation between foraminifer preservation and Fe and Ca, and thus we interpret variations in Fe as a proxy for terrigenous flux.

Ti/Al ratios are commonly used to determine the relative contributions of detrital material from fluvial and aeolian sources, as Ti is often associated with coarser size fractions delivered by aeolian processes and Al with small, clay-sized material carried to sea as suspended sediment (e.g., Govin et al., 2012; Ziegler et al., 2009).

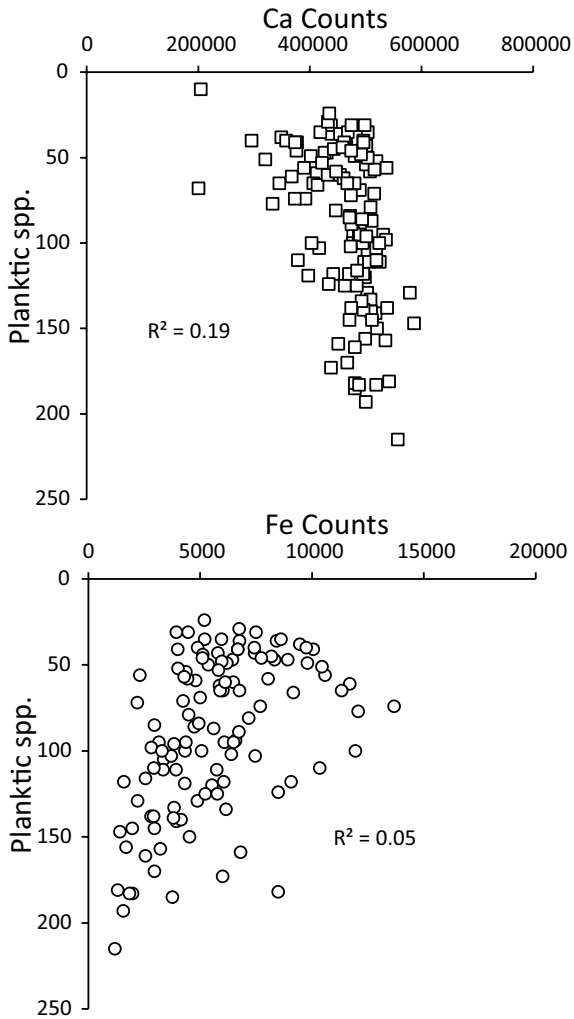

Figure 5. Preservation versus calcium and iron XRF counts. Better preservation is toward zero on the *y*-axis (i.e., fewer unidentifiable foraminifera). Two outliers >80,000 from pyrite-rich samples at the base of the section were removed from the Fe plot. Ca shows a weak negative correlation with good preservation while Fe shows a weak positive correlation with good preservation. This pattern is the opposite of trends caused by dissolution.

Large variations in terrigenous flux are evident in the Paleocene interval of Site M0077 (Figure 4). Overall, terrigenous flux (as measured by Fe and magnetic susceptibility) was low for the first ~1 Myr (to ~614 mbsf) of the Danian and higher thereafter. Numerous shorter peaks are superimposed on this long-term trend. It should be noted that the closest land was >800 km to the west in modern central México (Gulick et al., 2019), and thus terrigenous material only slightly diluted the pelagic carbonate at Site M0077. Ti/Al is positively correlated with Fe (Figure 4), indicating that intervals of increased terrigenous flux to Site M0077 were driven by periods of enhanced aeolian input to the Gulf of Mexico.

3.3. Water Column Structure

Planktic foraminiferal paleoecology provides insight into local hydrography. Planktic foraminifera occupy specific depth habitats in open ocean environments which can be determined via single-species isotopic analysis (e.g., Aze et al., 2011; Birch et al., 2012; Norris, 1996; Olsson et al., 1999). The pervasive foraminiferal recrystallization throughout Site M0077 prevents this kind of geochemical analysis, but fortunately published single-species isotope data exists for nearly every early Paleocene species (Table 2). The use of planktic foraminifer populations to reconstruct water column stratification is fairly common, particularly the relative abundance of deeper dwelling taxa (e.g., Boersma et al., 1987; D'Onofrio et al., 2016; Leckie et al., 2002; Pearson et al., 1993, 2006). Here, we use the proportion of mixed layer, thermocline, and sub thermocline taxa to reconstruct the degree to which the water column was stratified (Figure 6a). Dominance of mixed layer taxa indicates the lack of a suitable habitat for thermocline/subthermocline species, likely due to weak stratification, while higher abundances of thermocline and subthermocline species indicate stronger water column stratification creating a suitable deep habitat.

Overall, assemblages at Site M0077 are dominated by mixed layer taxa for the first ~200 kyr of the Danian. This is followed by a shift to more stratified waters from ~200-400 kyr (616.3–615.9 mbsf) after the K-Pg boundary, a return to a stronger mixed-layer water column from 400–900 kyr (615.9–614.9 mbsf) after the boundary, and finally a more permanent shift toward stable stratified waters after 900 kyr (above 614.9 mbsf) (Figure 6a).

3.4. Export Productivity

3.4.1. Export Production Terminology

Export production, the removal of organic matter from the euphotic zone to the deep sea, is primarily driven by the biological pump, in which carbon is moved downward via biological pathways like sinking organic matter, fecal pellets, the daily vertical migration of plankton, etc. (Zhang et al., 2018). The pump is usually described as having two parts: the export of net primary production out of the euphotic zone (~100 m depth) and the scavenging and remineralization of that organic carbon as it sinks to the seafloor, or at least deep enough to be removed from the short-term carbon cycle (~1,000 m depth) (e.g., Boyd & Newton, 1995; Boyd & Trull, 2007; Buessler, 1998; Buesseler & Boyd, 2009; Hilting et al., 2008; Henson et al., 2012; Legendre & Rivkin, 2002). Site M0077 was at ~700 m water depth in the early Danian (Lowery et al., 2018) but sediments which reached the seafloor and were buried can also be safely considered to be removed from the short-term carbon cycle. The amount of organic matter exported from the euphotic zone is often referred to as "export efficiency" (e.g., Buesseler & Boyd, 2009) or pump "strength" (e.g., Henson et al., 2012), and the

Table 2
Planktic Foraminifer Depth Habitat Assignments Based on the Ecogroups of Aze et al. (2011) Unless Otherwise Noted

Aze et al. (2011) ecogroups	Group	Explanation	Members
Group 1	Open ocean mixed-layer tropical/ subtropical, with symbionts	Very heavy $\delta^{13}C$ and relatively light $\delta^{18}O$	*Morozovella, Igorina, Acarinina, Praemurica inconstans*[c], *Preamurica pseudoinconstans*[c], *Praemurica uncinata*[c]
Group 2	Open Ocean mixed-layer tropical/ subtropical, without symbionts	$\delta^{13}C$ lighter than species with symbionts; also relatively light $\delta^{18}O$	*Guembelitria*[a], *Parvularugoglobigerina*[a], *Woodringina*[a], *Globoconusa daubjergensis*[a,b], *Rectuvigerina cretacea*[a], *Praemurica taurica*, *Subbotina triangularis*,
Group 3	Open Ocean thermocline	Light $\delta^{13}C$ and relatively heavy $\delta^{18}O$	*Globanomalina, Eoglobogerina Parasubbotina varianta, Subbotina trivialis, Subbotina triloculinoides*
Group 4	Open Ocean sub-thermocline	Very light $\delta^{13}C$ and very heavy $\delta^{18}O$	*Chiloguembelina midwayensis*[a], *Chiloguembelina morsei*[d], *P. pseudobulloides*
Group 5	High Latitude	Species only found in high latitude sites	N/A
Group 6	Upwelling/high productivity	Species only found in sites of high productivity or upwelling	N/A

Note. No taxa assigned to Groups 5 and 6 appear in our data set.
[a]Olsson et al. (1999) and references therein. [b]Olsson et al. (1999): Although its abundance in near-shore sequences indicates a near-surface planktic habitat (Keller, 1989; Liu & Olsson, 1992; Troelsen, 1957), its oxygen isotopic signature and open-marine abundance patterns suggest a preference for relatively cool water masses (Boersma & Silva, 1989; D'Hondt & Keller, 1991; D'Hondt & Zachos, 1993; Liu & Olsson, 1992). [c]Norris (1996) and Birch et al. (2012) describe *P. inconstans, P. pseudoinconstans,* and *P. uncinata,* as symbiont-bearing. [d]No isotope data are available for any other Paleocene Chiloguembelinids, so we place *Ch. morsei* in this group based on the data from its cousin *Ch. midwayensis*.

amount of organic matter that sinks below 1,000 m is called "transfer efficiency" (Buesseler & Boyd, 2009) or pump "efficiency" (Henson et al., 2012); here we opt to use the terms pump strength and efficiency (Henson et al., 2012). These two mechanisms are both part of the biological pump, and together they control the amount of organic matter removed from the euphotic zone to the deep sea, termed export production.

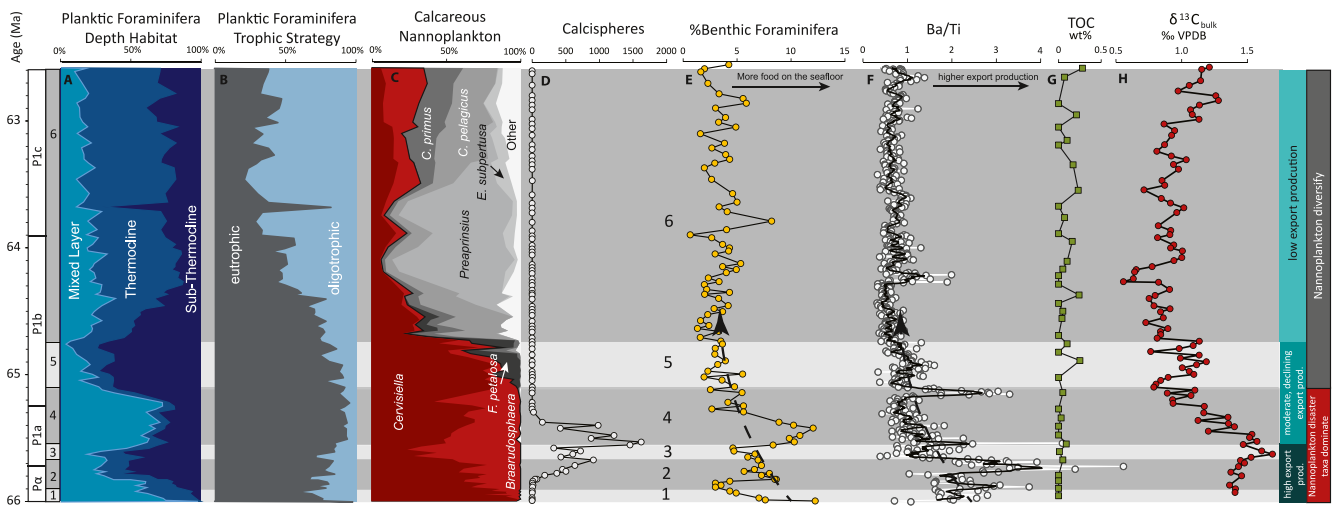

Figure 6. Paleoceanography proxies plotted by age. Planktic foraminifer by depth habitat (a) record the stratification of the upper water column; see Table 2 for species assigned to mixed layer, thermocline, and subthermocline planktic foraminifer groups. Planktic foraminifera by trophic strategy (b) record changes in paleoproductivity in the upper water column. Calcareous nannoplankton diversity (c) shows the relative abundance of all (non-reworked) species of calcareous nannoplankton present; red taxa are the so called "disaster" opportunists, gray are incoming Paleocene taxa. Calcispheres (d) shows the abundance of calcispheres >45 μm. %Benthics (e) is the percentage of benthic foraminifera relative to all foraminifera, and is interpreted to correspond primarily to abundance and quality of nutrient flux to the seafloor. Ba/Ti (f) records paleoproductivity, with high ratios indicating high productivity; white dots are individual data points, black lines is 5 point moving average. Total organic carbon (g) corresponds to changes in preservation potential of organic carbon at the seafloor. $\delta^{13}C_{bulk}$ (h) shows bulk rock stable carbon isotopes relative to the Vienna Pee Dee Belemnite (VPDB) standard. Numbered gray bars represent discrete intervals discussed in Section 4 of the text. Overall intervals of high, moderate, and low export productivity and nannoplankton diversity are shown on the right.

We use a range of proxies to reconstruct different parts of the biological pump, explained below. Barium is the most robust of these, and tracks overall export production from the eutrophic zone to the ocean interior (e.g., Griffith & Paytan, 2012).

3.4.2. The Barium Export Productivity Proxy

Biogenic barium, primarily preserved in marine sediments as barite ($BaSO_4$), strongly correlates with modern export production (Dymond et al., 1992; Eagle et al., 2003; Francois et al., 1995; Paytan & Griffith, 2007) and is thus a commonly used as an export productivity proxy (e.g., Paytan et al., 1996; Bains et al., 2000; Griffith & Paytan, 2012). Barite is primarily formed in marine environments during the remineralization of sinking organic matter below the euphotic zone, but it can also be sourced from terrigenous sediments. Therefore, barium is normalized to the terrestrially sourced element titanium (Dymond et al., 1992; Paytan & Griffith, 2007). This Ba/Ti "excess barium" proxy has been used to reconstruct export production in the early Paleocene using XRF data (Hull & Norris, 2011).

Different continental drainage basins may have differing Ba/Ti ratios, and thus long-term changes in sediment source area or dust versus riverine flux may complicate interpretation of the Ba/Ti export productivity proxy (Paytan & Griffith, 2007). However, significant changes in the sediment source to the southern Gulf of Mexico did not occur until the Laramide Orogeny, which began in the late Paleocene (Galloway et al., 2000) and therefore would not have influenced early Paleocene sedimentation. Shorter term sedimentation changes related to impact-driven land denudation (e.g., Tschudy et al., 1984) were on the order of 8–20 kyr (Vajda et al., 2004), too brief to explain the trends we observe. Another possible source of barium at Chicxulub is from the crater hydrothermal system, which was active throughout our study interval and which caused the precipitation of secondary barite in pore fluids in the underlying impact breccia (Kring et al., 2020). We also regard this as an unlikely source of Ba enrichment in the pelagic Paleocene sediments because secondary barite is only observed in the impact breccia, meters below the contemporary Danian seafloor (Kring et al., 2020). Additionally, Ba is only enriched in the lower few meters of the post impact sediments, while other hydrothermal elements are enriched throughout our study interval, indicating that the hydrothermal venting was active for millions of years after the crater formed (Kring et al., 2020) and that Ba was not supplied to the seafloor by this mechanism.

3.4.3. Foraminifer Export Proxies

While Ba/Ti ratios can tell us about the overall strength and efficiency of the whole biological pump, foraminifer ecology can help us understand some of its component parts. Planktic foraminifera live in the upper water column and record conditions related to primary production, among other water column properties. In the early Danian, some new genera (*Eoglobigerina* and the Subbotinids) evolved spines, long protrusions of calcite which provide an anchor for rhizopods (i.e., feeding appendages) and allow them to hold on to motile prey, enabling these groups to adapt a carnivorous lifestyle and graze upon other zooplankton (Hemleben et al., 1991; Olsson et al., 1999). This may have been an adaptation to a proliferation of smaller phytoplankton immediately after the extinction, whose small size would have made them a difficult food source for non-filter-feeders like planktic foraminifera; this would have promoted predation by foraminifera on other heterotrophs better adapted to eating such small autotrophs. Gibbs et al. (2020) found that mixotrophic nannoplankton were likely taking advantage of a similar niche (i.e., predation on tiny prey groups) which persisted well beyond the immediate aftermath of the extinction. On the other hand, microperforate and smooth normal perforate planktic foraminifera (in the Paleocene, these include *Guembelitria, Globoconusa, Parvularugoglobigerina, Woodringina, Chiloguembelina,* etc.) are unable to eat zooplankton, which are generally able to free themselves from unsupported rhizopodal networks; these foraminifera are primarily grazers, feeding on (larger) phytoplankton and any organic detritus that drifts by (Hemleben et al., 1991). Spinose planktic foraminifera are better adapted to food-limited environments, and should be predominant in oligotrophic waters (e.g., Hemleben et al., 1991). On the other hand, non-spinose, non-symbiont bearing planktics, the grazers, are best adapted to eutrophic environments, and should be dominant there.

Benthic foraminifera are also powerful paleoenvironmental indicators. They are primarily sensitive to changes in dissolved oxygen and food supply (Jorissen et al., 1995; Gooday, 2003; Van Hinsbergen

et al., 2005), and benthic foraminiferal abundance is also often inversely correlated with water depth (e.g., Alegret et al., 2020; Culver, 1988; Herguera & Berger, 1991; Leckie and Olson, 2003; Murray, 1976; Van der Zwaan et al., 1990). The seafloor at Site M0077 was well-oxygenated throughout the study interval as evidenced by abundant ichnofauna (Morgan et al., 2017; Rodriguez Tovar et al., 2020). The site was located in middle bathyal depths (600–700 m; Gulick et al., 2008; Lowery et al., 2018), and low-amplitude sea level change throughout the early Paleocene (e.g., Miller et al., 2020) should not have affected the %benthics at this depth. With changes in oxygen and sea level thus ruled out, we are confident that food supply to the seafloor (i.e., export production) was the strongest influence on %benthics at Site M0077. %Benthics may reflect changes in either the quantity or the quality (i.e., labile vs. refractory) of the organic matter that reached the seafloor (e.g., Jorissen et al., 1995).

3.4.4. Early Paleocene Trends in Export Productivity

Export productivity, indicated by Ba/Ti, was high overall in the early Danian, and broadly declined over the first ~1.2 Myr post impact (616.5–~614.1 mbsf) (Figure 6f). The interval of highest export productivity terminated sharply around 300 kyr post impact (616.2 mbsf). The subsequent period of decline is interrupted by a second peak in export production which occurred 800 kyr post-impact (615.1 mbsf), after which export production flattened out. These trends are mirrored in the foraminifera populations. Benthic foraminifera were more abundant overall in the early Danian (Figure 6e), indicating either higher export of organic matter to the seafloor overall or a relatively large proportion of labile organic matter being exported. Likewise, non-spinose, non-symbiont-bearing planktic foraminifera were more abundant in the early Danian (Figure 6b). This dominance is not an artifact of post-extinction communities being composed of only non-spinose foraminifera. Spinose foraminifera appeared essentially immediately after the extinction: the lowest occurrences of *Eoglobigerina* and *Parasubbotina* are in Zone P0, while that of *Subbotina* occurs early in Zone P1a, ~300 kyr after the boundary, indicating that an evolutionary advantage conferred by spines existed in at least some parts of the ocean soon after the impact. The abundance of non-spinose foraminifera suggests that there was abundant food for grazers at this particular location; the decline in spinose taxa over the first 900 kyr after the impact implies an increase in larger, more easily grazed phytoplankton over this time, further reducing the advantages of carnivory at this place and time. Although not directly correlated with export productivity as indicated by Ba/Ti, these foraminifer proxies provide additional context on the state of different aspects of the biological pump.

After 1.2 Myr post-impact the study interval is characterized by low and stable Ba/Ti ratios (with several small short-lived increases) paired with an increase in nannoplankton diversity. This increase in diversity is characterized by a series of nannoplankton acme events featuring higher abundances of oligotrophic taxa like *Coccolithus primus* and *Cruciplacolithus pelagicus,* which indicate fewer nutrients in the euphotic zone (Figure 6c) (Jones et al., 2019). At the same time, fewer benthic foraminifera indicate decreased food supply to the seafloor.

4. Paleoceanographic Evolution of the Chicxulub Crater

Collectively, our data indicate a shift from high export productivity and weak stratification in the earliest Paleocene to low export productivity and strong stratification a few million years later. The change between these two regimes also marks a shift in the phytoplankton community. This progression occurs in several steps (see numbered, shaded bars on Figure 6) detailed below.

4.1. High Export Productivity, Well-Mixed Water Column (0–100 kyr Post Impact)

The first 100 kyr after the Chicxulub impact (616.5–616.4 mbsf; interval 1 on Figure 6) were characterized by high export production and were dominated by mixed-layer planktic foraminifera, predominantly *Guembelitria, Globoconusa,* and *Parvularugoglobigerina*, while the calcareous dinoflagellate disaster taxon *Cervisiella* dominated the nannoplankton size fraction. Schaefer et al. (2020) used biomarkers to document the presence of cyanobacteria in this interval, while Bralower et al. (2020a) found micritic fossils with a number of morphological features which strongly resemble calcareous cyanobacteria grown in culture. Bralower et al. (2020a) attributed the micrite layer just above the K-Pg boundary at Chicxulub and numerous other sites to "whitings" caused by blooms of calcareous cyanobacteria in the aftermath of the extinction. Several

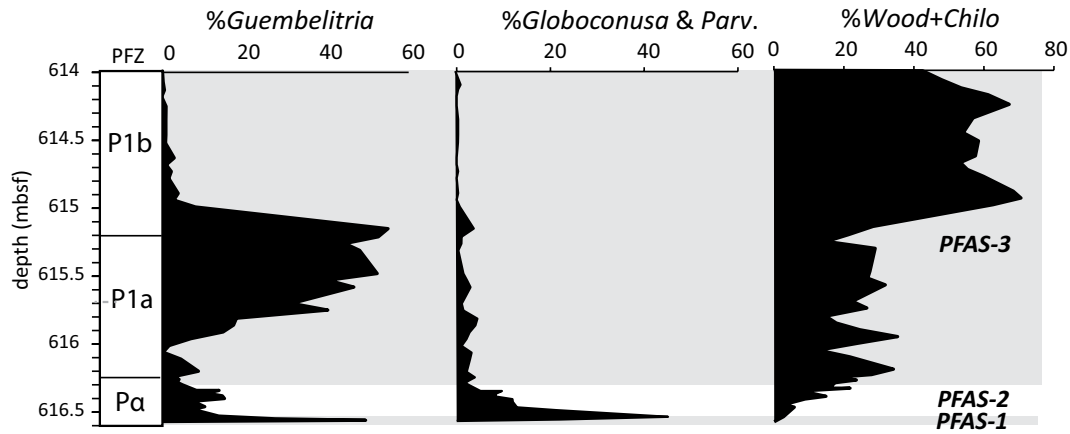

Figure 7. Quantitative stratigraphic distribution of early Danian planktic foraminiferal groups at Site M0077 and Planktic Foraminiferal Acme Stages (PFAS) 1–3: PFAS-1 is the predominance of *Guembelitria*, PFAS-2 is the predominance of *Parvularugoglobigerina* and *Globoconusa* (or *Palaeoglobigerina* according to Arenillas & Arz, 2017), and PFAS-3 is the predominance of *Woodringina* and *Chiloguembelina*. A second acme of *Guembelitria* (or *Chiloguembelitria* according to Arenillas & Arz, 2017) occurs within this stage across the Tethys, as is also evident at Site M0077.

acmes of planktic foraminifera occurred across the Tethys and North Atlantic after the K-Pg boundary, termed Planktic Foraminiferal Acme Stages (PFAS; Arenillas et al., 2000, 2006, 2016; Alegret et al., 2004). These represent a coeval succession of dominant taxa in open marine sections over a wide geographic area. PFAS-1, the predominance of *Guembelitria*, occurs in this earliest interval of post-impact sedimentary rocks (Figure 7).

4.2. Very High Export Productivity, Increasing Stratification (100–320 kyr Post Impact)

During the period from 100–320 kyr after the impact (616.4–616.1 mbsf; interval 2 on Figure 6), export productivity peaked, benthic foraminifer abundance increased, and thermocline and sub-thermocline dwelling foraminifera (*Eoglobigerina* and *Chiloguembelina*) became more common. This transition is coincident with a small increase in terrigenous flux (Figure 4). PFAS-2, the predominance of *Globoconusa* and *Parvularugoglobigerina*, occurs in this interval (Figure 7). The nannoplankton size fraction was still dominated by the resting cysts of calcareous dinoflagellates (*Cervisiella*).

4.3. Declining Export Productivity, Well Stratified Water Column (320–400 kyr Post Impact)

A sharp decrease in export productivity occurred ~320 kyr after the boundary (616.1 mbsf; interval 3 on Figure 6) in the middle of a period of well-developed water column stratification. *Braarudosphaera* became predominant in the nannoplankton size fraction as *Cervisiella* declined, but this is coincident with an increase in foraminifer-sized calcispheres (Figure 6), suggesting a shift toward dominance of a larger calcareous dinoflagellate taxon rather than an overall decrease in their abundance. Liebrand et al. (2018) found *Braarudosphaera* oozes associated with hyperstratification during the Oligocene. This interpretation matches with the increase in stratification we observe with planktic foraminifera at Site M0077. PFAS-3, the predominance of *Woodringina* and the sub-thermocline-dwelling *Chiloguembelina*, also begins in this interval.

4.4. Moderate Export Productivity, Poorly Stratified Water Column (400–900 kyr Post Impact)

Around 400 kyr after the impact (615.9 mbsf; interval 4 on Figure 6), water column stratification weakened and mixed layer taxa again dominated the planktic foraminiferal assemblage. Benthic foraminifera reached their peak abundance, perhaps indicating an increase in labile organic matter arriving at the seafloor. Foraminifer-sized calcispheres peaked and then declined as *Cervisiella* again came to dominate the

Table 3
Post K-Pg Changes in Export Production at Different Sites

Location	Proxy	Increase in export production 300 kyr post K-Pg?	Reference
Western Gulf of Mexico	Benthic forams	Yes	Alegret et al. (2001); Alegret and Thomas (2005)
Spain	Benthic forams	Yes	Alegret and Thomas (2005)
Gubbio	Benthic forams	Yes	Coccioni et al. (2010)
Maud Rise	Ba	Yes	Hull and Norris (2011)
Shatsky Rise	Ba	Yes	Hull and Norris (2011)
Walvis Ridge	Planktic forams	Yes	Birch et al. (2016)
Vigo Seamount	Ba	No change	Hull and Norris (2011)
Sao Paulo Plateau	Ba	No change	Hull and Norris (2011)
Wombat Plateau	Ba	No change	Hull and Norris (2011)

nannofossil size fraction (Jones et al., 2019). Export productivity continued its decline from its earlier peak but was still relatively elevated compared to subsequent values.

4.5. Productivity Completes Its Decline, Stratification Redevelops (900–1,200 kyr Post Impact)

Over the next ~300 kyr (614.9–614.1 mbsf; interval 5 on Figure 6) stratification gradually strengthened while export productivity slowly declined following a final large peak just below this interval. The termination of this peak in Ba/Ti is associated with the onset of the first acme of incoming Paleocene nannoplankton, *Futyania petalosa*, 900 kyr after the K-Pg boundary; the lowest appearances of *Cruciplacoluthis primus* and *Coccolithus pelagicus* soon follow (Jones et al., 2019). *F. petalosa* became more abundant throughout this interval, in conjunction with a continued decline in Ba/Ti values.

4.6. Low Export Productivity, Stable, Stratified Water Column (>1,200 kyr Post Impact)

The rest of the lower Paleocene record at Site M0077 (614.1–610.6 mbsf; interval 6 on Figure 6) documents a stable, stratified, increasingly oligotrophic environment. A stepped decline in Ba/Ti at the base of this interval is associated with the increased abundance of *C. primus* and then that of *C. pelagicus* a few hundred thousand years later (Jones et al., 2019). Following the *Praeprinsius* acme, which terminates around 63.5 Ma (Jones et al., 2019), no further acmes occur, indicating that the post-extinction ecosystem was finally stabilized. Ba/Ti ratios are essentially steady through this interval.

5. What Drove the Decline in Export Production?

A clear change in export productivity occurs ~300 kyr after the K-Pg boundary at many sites around the globe, although the direction of the change varies locally (Table 3). These sites are broadly distributed geographically and represent a range of depositional environments. The lack of globally consistent shifts in productivity may be considered analogous to patterns during other major paleoceanographic events, like the Paleocene Eocene Thermal Maximum (e.g., Gibbs et al., 2006) or Oceanic Anoxic Event 2 (Tsikos et al., 2004), in which local signals often differ significantly from the global "average" change. An important question, then, is what caused these local to regional changes?

5.1. Hypothesis 1: Recovery of the Marine Ecosystem

One explanation for the widespread coeval shifts in export productivity around 300 kyr after the K-Pg is the gradual recovery of marine ecosystems after a major mass extinction event. In this hypothesis, changes in the plankton ecosystem drove changes in the local biological pump and explain regional patterns of export productivity change. Plankton ecology is the single most important control on the strength and efficiency of the biological pump (e.g., Henson et al., 2012). In the modern ocean, net primary production (NPP) driven by large-celled phytoplankton like diatoms and coccolithophores results in a stronger biological

pump and thus higher export production (e.g., Boyd, 2015; Boyd & Newton, 1995, 1999; Boyd & Trull, 2007; Buessler, 1998; Lam et al., 2011; Legendre & Rivkin, 2002). Primary production by smaller-celled picophytoplankton like cyanobacteria and some algae sinks more slowly and is more easily remineralized in surface waters (the "microbial loop"); in regions where picoplankton dominate primary production, nutrients are constantly recycled at shallow depth and export production is primarily composed of more refractory organic matter which is resistant to degradation as it sinks through mesopelagic depths (de la Rocha & Passow, 2007). Counterintuitively, even though the biological pump is *weaker* when primary production is dominated by picoplankton (less organic matter is exported from the euphotic zone), it is *more efficient* (a larger proportion of the organic matter that is exported from the euphotic zone safely sinks to the seafloor because it is more refractory). On the other hand, larger-celled phytoplankton like coccolithophores and diatoms sink more quickly, and in regions where they dominate, more organic matter is exported from the euphotic zone. However, this has the effect of increasing the amount of labile organic matter sinking through intermediate depths to be remineralized by grazers there, so although the biological pump is *stronger* (more organic carbon is exported from the euphotic zone), it is *less efficient* (a smaller proportion of the organic carbon that makes it out of the euphotic zone safely sinks to the seafloor). The abundance of larger phytoplankton has the net effect of removing organic matter and nutrients from the euphotic zone but not exporting it efficiently to the seafloor. For example, Henson et al. (2012) document a strong, inefficient biological pump at high latitudes driven by diatoms, in which 15%–25% of NPP sinks below the euphotic zone but only 1%–10% of that material reaches 2,000 m water depth. On the other hand, they describe a weak, efficient pump at low latitudes driven by small-celled phytoplankton, where only 1%–5% of NPP is exported out of the euphotic zone but 20%–35% of that proportion makes it to 2,000 m. (It should be noted that there is still no clear consensus on these trends in the modern ocean; see Marsay et al., 2015 or Weber et al., 2016.)

After the K-Pg mass extinction, the dominant larger-celled phytoplankton of the Cretaceous, calcareous nannoplankton, declined severely (Bown et al., 2004). Primary production was carried on by picoplankton like chlorophyte algae (Sepúlveda et al., 2009) and cyanobacteria (Bralower, Cosmidis, Heaney et al., 2020; Schaefer et al., 2020); the dominance of these small groups weakened the biological pump. In some oligotrophic regions, the shift toward picoplankton and enhanced recycling of nutrients in the euphotic zone may have actually driven a local increase in primary productivity (see discussion in Henehan et al., 2019). If the southern Gulf of Mexico was one of these regions, then a dominance of picoplankton would explain our observation of high export productivity in the immediate aftermath of the extinction. The subsequent recovery of calcareous nannoplankton as important contributors to primary production would have facilitated a higher removal of nutrients from the euphotic zone, causing the observed local shift from eutrophic to oligotrophic conditions.

5.2. Hypothesis 2: Paleoceanographic Control

An alternative explanation for changes in export production that must be considered is some local or global oceanographic event. Perhaps changes in hydroclimate caused a change in terrigenous nutrient flux to the ocean. Or perhaps a shift in ocean circulation patterns caused a shift in thermal stratification and mixing processes which reduced nutrient delivery to the euphotic zone. Indeed, there are limited data in support of variations in stratification around 300 kyr post K-Pg, including at Walvis Ridge in the South Atlantic (Birch et al., 2016) and the Gubbio section in Italy (Coccioni et al., 2010). The Dan-C2 hyperthermal ends around this time (e.g., Barnet et al., 2019; Coccioni et al., 2010), and may conceivably be related. Unfortunately, the Dan-C2 hyperthermal itself is not observed at Site M0077, either because it is too condensed or because the carbonate stable isotopes have been altered during diagenesis, but in any case an oceanographic driver for the observed productivity trends, like changing stratification or terrigenous flux, should be considered.

5.3. Testing the Two Hypotheses

Thus, we have two hypotheses to explain the early Paleocene export productivity data at Site M0077: (a) increasing stratification and/or decreasing terrigenous nutrient flux reducing nutrient availability, or (b) initial dominance of picoplankton causing recycling of nutrients in the euphotic zone and increased export efficiency, followed by a recovery of larger celled phytoplankton enhancing export of nutrients and organic matter from the euphotic zone, reducing primary production and making the pump less efficient. Testing

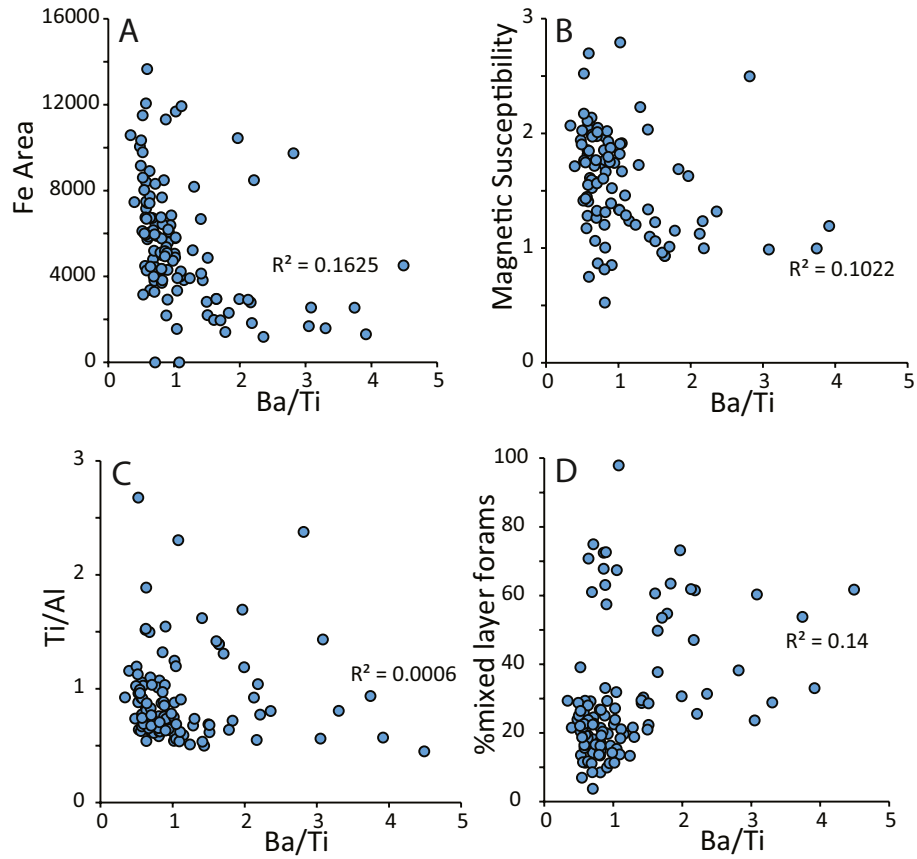

Figure 8. Cross plots of Ba/Ti ratios (i.e., export productivity) with proxies for stratification and terrigenous flux: (a) XRF Fe counts, a proxy for sedimentary dilution by terrigenous sediments, (b) magnetic susceptibility, a proxy for the influx of terrigenous material, (c) Ti/Al, a proxy for the relative abundance of aeolian (Ti) versus riverine (Al) flux, (d) the percent abundance of mixed layer foraminifera versus total foraminifera, a proxy for the vertical stratification of the upper water column. R^2 values (and your eyeballs, probably) indicate that all four are uncorrelated and thus changes in export productivity were not related to terrigenous flux or water column stratification.

the latter hypothesis would require data on the relative abundance of groups of phytoplankton which do not usually leave body fossils, like algae and cyanobacteria, and such data do not currently exist for any early Paleocene section (Schaefer et al., 2020; Sepúlveda et al., 2009, 2019). Biomarker data from the Chicxulub crater do indicate a presence of cyanobacteria in the first few 100 kyrs after the K-Pg Boundary (Schaefer et al., 2020), corresponding to the interval of the highest export production and thus providing some support for the hypothesis that plankton ecology drove the observed changes. Bralower, Cosmidis, Heaney et al. (2020) also found evidence of global acmes of microbial phytoplankton, presumed to be cyanobacteria, associated with the widespread deposition of microcrystalline calcite above the K-Pg boundary, indicating cyanobacteria blooms caused whitings at many localities (including the Chicxlub crater). Moreover, Alvarez et al. (2019) found an increase in average nannoplankton cell size coincident with the initial increase in diversity at Shatsky Rise in the equatorial Pacific, indicating connection between increased nannoplankton cell size and the recovery of the biological pump at this site. However, without detailed plankton biomarker data we only have an incomplete picture of the potential phytoplankton community and cannot directly test this hypothesis.

We can, however, test the alternate hypothesis (that oceanographic changes drove a decline in export productivity) by determining if there is a correlation between proxies for stratification and/or terrigenous flux and export productivity in the Chicxulub crater. Figure 8 is a series of cross plots showing the lack of correlation between export productivity indicated by Ba/Ti ratios and proxies for stratification and terrigenous flux. Figures 8a and 8b compare two proxies for overall terrestrial input, total Fe and magnetic susceptibility,

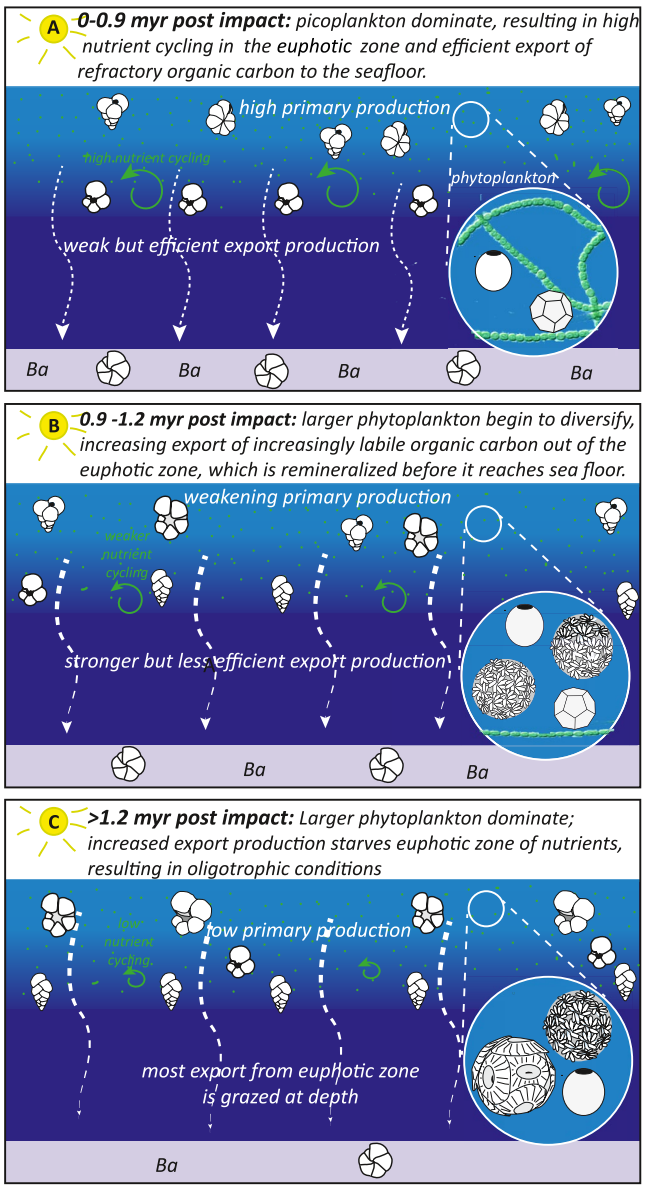

Figure 9. Summary of interpreted ecological and paleoproductivity changes over the study interval at IODP Site M0077. (a) Picoplankton, including cyanobacteria, dominate the primary producing ecosystem while calcareous nannoplankton and dinocysts are less abundant. Small phytoplankton sink slowly and result in high nutrient cycling in the euphotic zone, fueling high productivity in the euphotic zone and efficient export production because refractory organic matter is more likely to survive sinking to the seafloor, feeding benthic foraminifera and enriching sediments in biogenic Ba. (b) Calcareous nannoplankton begin to become more abundant and diverse and picoplankton decline; larger phytoplankton mean increased export of organic matter from the euphotic zone, which reduces the recycling of nutrients, reducing primary productivity. This material also tends to be more labile and therefore more easily scavenged, thereby reducing flux of organic matter to the sea floor. (c) As calcareous nannoplankton recovery nears completion, increased export of organic matter from the euphotic zone results in oligotrophic conditions in surface waters (spurring an increase in oligotrophic-adapted planktic foraminifera) and reduced flux of organic matter to the seafloor.

with export productivity; both clearly show no trend. Figure 8c compares the ratio of Ti to Al, which tracks shifts in aeolian versus riverine input (e.g., Govin et al., 2012) with export productivity. There are clear shifts in the Ti/Al ratio (Figure 4) coincident with shifts in Fe, indicating that shifts between wetter and drier climate states drove changes in the delivery of terrigenous elements to Site M0077. However, when plotted against Ba/Ti, it is clear that such shifts in sediment source have no bearing on export productivity. Another possibility is that nutrients were sourced from depth, and a weakly stratified water column (facilitating upwelling) enhanced export production. Figure 8d compares the percentage of mixed layer planktic foraminifera with Ba/Ti to test this idea, and convincingly demonstrates that changing stratification was unrelated to export productivity. It is possible that seasonal breakdowns in stratification caused brief blooms of phytoplankton which dominate the total signal, while planktic foraminifer populations record longer periods of stable stratification the rest of the year. Such changes are beyond the resolution of current paleoceanographic proxies for the Paleocene and cannot be ruled out. However, this explanation would still require some physical change in the study area affecting seasonal upwelling (changes in temperature, perhaps, or terrigenous flux), and because no such driver is evident in our data, we consider this explanation to be unlikely.

Another possibility that must be addressed is the effect of temperature on metabolic rates of grazers, with warmer waters facilitating increased remineralization of sinking organic matter, essentially making the biological pump less efficient (e.g., Boscolo-Galazzo et al., 2021; Griffith et al., 2021). Unfortunately, pervasive diagenetic alteration of carbonates means that it is not possible to make meaningful interpretations of temperature trends at Site M0077 using the bulk carbonate oxygen isotope record. However, we know that temperatures were predominantly warm and stable throughout the Danian, with the only departure being the few degrees C of warming associated with the Dan-C2 event. Griffith et al. (2021) examined changes in benthic foraminifera and barium flux across Eocene hyperthermals and found that warming caused increased remineralization of organic matter below the euphotic zone, recorded as an increase in Ba and a decline in benthic foraminifera. Unfortunately, the characteristic carbon isotope excursion associated with the Dan-C2 hyperthermal cannot be identified in our core, likely due to both the aforementioned diagenetic alteration and slow sedimentation rates. Given the broadly stable global temperatures of our study interval we conclude that temperature change was not a major driver of the observed patterns of export production at Site M0077.

Finally, it could be argued that a post-extinction decline in grazers below the euphotic zone temporarily caused a larger-than-usual proportion of net primary production to safely sink through that depth interval to be exported, and that a recovery of grazers is responsible for the subsequent decline of export production. However, the abundance and diversity of planktic foraminifera immediately after the K-Pg boundary argue against this. Foraminifera are certainly not the most abundant or important grazers in the modern ocean, but they are the only ones well-represented in the fossil record and so can serve as a good proxy for this broader group. Additionally, Bralower, Cosmidis, Fantle et al., (2020) found fossil evidence of copepods immediately above the boundary layer at Site M0077.

All this would seem to suggest that grazers were an active part of the earliest Paleocene ecosystem and thus do not explain the observed trends in export production

In summary, we favor the hypothesis that turnover in phytoplankton communities from picophytoplankton like cyanobacteria to larger phytoplankton like coccolithophores drove a strengthening of the biological pump, which removed nutrients in the euphotic zone and caused a decline in export production. This explanation is summarized in Figure 9. Biomarker-based studies of the whole plankton ecosystem from multiple early Paleocene sites are necessary to fully test this hypothesis.

6. Conclusions

The earliest Danian oceanic environment is often referred to as generally "unstable" (e.g., Alegret et al., 2003; Culver and Buzas, 2000; Hull et al., 2011). Our data from Site M0077 in the Chicxulub crater suggest that at least one component of this instability is a fluctuating degree of water column stratification. Water column stratification varied widely over the first ~ million years of the Paleocene, but with an overall trend from poorly stratified to well stratified. Export productivity varied over the same interval, with an overall decreasing trend. There is no strong correlation between proxies for stratification or terrigenous flux with export productivity. Instead, we suggest that the decline in export productivity was linked to turnover in the phytoplankton community, as post-impact acmes of cyanobacteria (Bralower, Cosmidis, Heaney et al., 2020; Schaefer et al., 2020) and other non-fossilizing picophytoplankton gave way to larger calcareous nannoplankton. Data from Site M0077 support this plankton ecology hypothesis, with a dominance of cyanobacteria (Bralower, Cosmidis, Heaney et al., 2020; Schaefer et al., 2020) during the interval of highest export production, and recovery of calcareous nannoplankton diversity as export production declines. However, more complete biomarker data on the rest of the non-fossilizing phytoplankton ecosystem at multiple K-Pg boundary sites are required to truly test this hypothesis.

Acknowledgments
We are grateful to Ellen Thomas, Julio Sepúlveda, and four anonymous reviewers for their constructive comments, which have substantially improved this work. The authors acknowledge NSF OCE 1737351, 1736951, and 1737199. We are grateful to Pincelli Hull for her helpful discussions on our data and hers, and to the staff of the Bremen Core Repository for their invaluable help sampling and scanning the core. We also thank Tessa Cayton for her assistance preparing foraminifer samples. I. Arenillas and J. A. Arz acknowledge the use of the Servicio General de Apoyo a la Investigación-SAI, Universidad de Zaragoza. The European Consortium for Ocean Research Drilling (ECORD) implemented Expedition 364 with funding from the International Ocean Discovery Program (IODP) and the International Continental Scientific Drilling Project (ICDP). Data and samples can be requested from IODP. U.S. participants in Expedition 364 were supported by the U.S. Science Support Program. J. Morgan was funded by NERC, grant: NE/P005217/1. I. Arenillas and J. A. Arz were supported by MINECO/FEDER-UE (project number CGL2015-64422-P) and MCIU/AEI/FEDER, UE (project number PGC2018-093890-B-I00). This is University of Texas Institute for Geophysics Contribution #3661 and Center for Planetary Systems Habitability Contribution #0023

Appendix A: Expedition 364 Science Party

Elise Chenot, Gail Christeson, Philippe Claeys, Charles Cockell, Marco J. L. Coolen, Ludovic Ferrière, Catalina Gebhardt, Kazuhisa Goto, Sophie Green, Kliti Grice, Sean Gulick, Heather Jones, David A. Kring, Johanna Lofi, Christopher M. Lowery, Claire Mellett, Joanna Morgan, Rubén Ocampo-Torres, Ligia Perez-Cruz, Annemarie Pickersgill, Michael Poelchau, Auriol Rae, Cornelia Rasmussen, Mario Rebolledo-Vieyra, Ulrich Riller, Honami Sato, Bettina Schaefer, Jan Smit, Sonia Tikoo, Naotaka Tomioka, Jaime Urrutia-Fucugauchi, Michael Whalen, Axel Wittmann, Long Xiao, Kosei Yamaguchi, William Zylberman.

Data Availability Statement

Planktic foraminifer data and XRF core scan data are archived at the NOAA National Centers for Environmental Information at https://www.ncdc.noaa.gov/paleo/study/34212. Calcareous nannoplankton data are from Jones et al. (2019) and are archived at https://doi.org/10.1130/2019271.

References

Agnini, C., Fornaciari, E., Raffi, I., Catanzariti, R., Pälike, H., Backman, J., & Rio, D. (2014). Biozonation and biochronology of Paleogene calcareous nannofossils from low and middle latitudes. Newsletters on Stratigraphy, 47, 131–181. https://doi.org/10.1127/0078-0421/2014/0042

Alegret, L., Arenillas, I., Arz, J. A., & Molina, E. (2004). Foraminiferal event-stratigraphy across the Cretaceous/Paleogene boundary. Neues Jahrbuch für Geologie und Paläontologie - Abhandlungen, 234, 25–50. https://doi.org/10.1127/njgpa/234/2004/25

Alegret, L., Arreguín-Rodríguez, G. J., Trasviña-Moreno, C. A., & Thomas, E. (2020). Turnover and stability in the deep sea: Benthic foraminifera as tracers of Paleogene global change. Global and Planetary Change, 103372.

Alegret, L., Molina, E., & Thomas, E. (2001). Benthic foraminifera at the Cretaceous-Tertiary boundary around the Gulf of Mexico. Geology, 29, 891–894. https://doi.org/10.1130/0091-7613(2001)029<0891:bfatct>2.0.co;2

Alegret, L., Molina, E., & Thomas, E. (2003). Benthic foraminiferal turnover across the Cretaceous/Paleogene boundary at Agost (southeastern Spain): Paleoenvironmental inferences. Marine Micropaleontology, 48(3–4), 251–279. https://doi.org/10.1016/s0377-8398(03)00022-7

Alegret, L., & Thomas, E. (2005). Cretaceous/Paleogene boundary bathyal paleo-environments in the central North Pacific (DSDP Site 465), the Northwestern Atlantic (ODP Site 1049), the Gulf of Mexico and the Tethys: The benthic foraminiferal record. Palaeogeography, Palaeoclimatology, Palaeoecology, 224, 53–82. https://doi.org/10.1016/j.palaeo.2005.03.031

Alegret, L., Thomas, E., & Lohmann, K. C. (2012). End-Cretaceous marine mass extinction not caused by productivity collapse. Proceedings of the National Academy of Sciences, 109(3), 728–732. https://doi.org/10.1073/pnas.1110601109
Alvarez, L. W., Alvarez, W., Asaro, F., & Michel, H. V. (1980). Extraterrestrial cause of the Cretaceous–Tertiary extinction. Science, 208, 1095–1108. https://doi.org/10.1126/science.208.4448.1095
Alvarez, S. A., Gibbs, S. J., Bown, P. R., Kim, H., Sheward, R. M., & Ridgwell, A. (2019). Diversity decoupled from ecosystem function and resilience during mass extinction recovery. Nature, 574(7777), 242–245. https://doi.org/10.1038/s41586-019-1590-8
Arenillas, I., & Arz, J. A. (2017). Benthic origin and earliest evolution of the first planktonic foraminifera after the Cretaceous/Paleogene boundary mass extinction. Historical Biology, 29, 17–24. https://doi.org/10.1080/08912963.2015.1119133
Arenillas, I., Arz, J. A., Grajales-Nishimura, J. M., Murillo-Muñetón, G., Alvarez, W., Camargo-Zanoguera, A., et al. (2006). Chicxulub impact event is Cretaceous/Paleogene boundary in age: New micropaleontological evidence. Earth and Planetary Science Letters, 249, 241–257. https://doi.org/10.1016/j.epsl.2006.07.020
Arenillas, I., Arz, J. A., Grajales-Nishimura, J. M., & Rojas-Consuegra, R. (2016). The Chicxulub impact is synchronous with the planktonic foraminifera mass extinction at the Cretaceous/Paleogene boundary: New evidence from the Moncada section, Cuba. Geológica Acta, 14(1), 35–51. https://doi.org/10.1344/GeologicaActa2016.14.1.4
Arenillas, I., Arz, J. A., Molina, E., & Dupuis, C. (2000). An independent test of planktic foraminiferal turnover across the Cretaceous/Paleogene (K/P) boundary at El Kef, Tunisia; catastrophic mass extinction and possible survivorship. Micropaleontology, 46, 31–49.
Artemieva, N., Joanna, M., & Expedition 364 Science Party. (2017). Quantifying the release of climate-active gases by large meteorite impacts with a case study of Chicxulub. Geophysical Research Letters, 44, 10180–10188. https://doi.org/10.1002/2017GL074879
Artemieva, N., & Morgan, J. (2020). Global K-Pg layer deposited from a dust cloud. Geophysical Research Letters, 47(6), e2019GL086562. https://doi.org/10.1029/2019gl086562
Aze, T., Ezard, T. H. G., Purvis, A., Coxall, H. K., Stewart, D. R. M., Wade, B. S., & Pearson, P. N. (2011). A phylogeny of Cenozoic macroperforate planktonic foraminifera from fossil data. Biological Reviews, 86, 900–927. https://doi.org/10.1111/j.1469-185x.2011.00178.x
Bains, S., Norris, R. D., Corfield, R. M., & Faul, K. L. (2000). Termination of global warmth at the Palaeocene/Eocene boundary through productivity feedback. Nature, 407, 171–174. https://doi.org/10.1038/35025035
Bardeen, C. G., Garcia, R. R., Toon, O. B., & Conley, A. J. (2017). On transient climate change at the Cretaceous—Paleogene boundary due to atmospheric soot injections. Proceedings of the National Academy of Sciences, 114(36), E7415–E7424. https://doi.org/10.1073/pnas.1708980114
Barnet, J. S., Littler, K., Westerhold, T., Kroon, D., Leng, M. J., Bailey, I., et al. (2019). A high--fidelity benthic stable isotope record of late Cretaceous–early Eocene climate change and carbon-cycling. Paleoceanography and Paleoclimatology, 34(4), 672–691. https://doi.org/10.1029/2019pa003556
Berggren, W. A., & Pearson, P. N. (2005). A revised tropical to subtropical Paleogene planktonic foraminiferal zonation. Journal of Foraminiferal Research, 35, 279–298. https://doi.org/10.2113/35.4.279
Birch, H., Schmidt, D. N., Coxall, H. K., Kroon, D., & Ridgwell, A. (2021). Ecosystem function after the K/Pg extinction: Decoupling of marine carbon pump and diversity. Proceedings of the Royal Society B, 288(1953), 20210863. https://doi.org/10.1098/rspb.2021.0863
Birch, H. S., Coxall, H. K., & Pearson, P. N. (2012). Evolutionary ecology of Early Paleocene planktonic foraminifera: Size, depth habitat and symbiosis. Paleobiology, 38(3), 374–390. https://doi.org/10.1666/11027.1
Birch, H. S., Coxall, H. K., Pearson, P. N., Kroon, D., & Schmidt, D. N. (2016). Partial collapse of the marine carbon pump after the Cretaceous-Paleogene boundary. Geology, 44, 287–290. https://doi.org/10.1130/g37581.1
Boersma, A., & Silva, I. P. (1989). Atlantic Paleogene biserial heterohelicid foraminifera and oxygen minima. Paleoceanography, 4, 271–286. https://doi.org/10.1029/pa004i003p00271
Boersma, A., Silva, I. P., & Shackleton, N. J. (1987). Atlantic Eocene planktonic foraminiferal paleohydrographic indicators and stable isotope paleoceanography. Paleoceanography, 2(3), 287–331. https://doi.org/10.1029/pa002i003p00287
Boscolo-Galazzo, F., Crichton, K. A., Ridgwell, A., Mawbey, E. M., Wade, B. S., & Pearson, P. N. (2021). Temperature controls carbon cycling and biological evolution in the ocean twilight zone. Science, 371(6534), 1148–1152. https://doi.org/10.1126/science.abb6643
Bown, P., & Young, J. R. (1998). Calcareous nannofossil biostratigraphy (pp. 1–15). Chapman and Hall; Kluwer Academic. https://doi.org/10.1007/978-94-011-4902-0_1
Bown, P. R., Lees, J. A., & Young, J. R. (2004). Calcareous nannoplankton evolution and diversity through time. In Coccolithophores (pp. 481–508): Springer. https://doi.org/10.1007/978-3-662-06278-4_18
Boyd, P., & Newton, P. (1995). Evidence of the potential influence of planktonic community structure on the interannual variability of particulate organic carbon flux. Deep Sea Research Part I: Oceanographic Research Papers, 42(5), 619–639. https://doi.org/10.1016/0967-0637(95)00017-z
Boyd, P. W. (2015). Toward quantifying the response of the oceans' biological pump to climate change. Frontiers of Marine Science, 2, 77. https://doi.org/10.3389/fmars.2015.00077
Boyd, P. W., & Newton, P. P. (1999). Does planktonic community structure determine downward particulate organic carbon flux in different oceanic provinces? Deep Sea Research Part I: Oceanographic Research Papers, 46(1), 63–91. https://doi.org/10.1016/s0967-0637(98)00066-1
Boyd, P. W., & Trull, T. W. (2007). Understanding the export of biogenic particles in oceanic waters: Is there consensus? Progress in Oceanography, 72(4), 276–312. https://doi.org/10.1016/j.pocean.2006.10.007
Bralower, T. J., Cosmidis, J., Fantle, M. S., Lowery, C. M., Passey, B. H., Gulick, S. P. S., et al. (2020). The habitat of the nascent Chicxulub crater. AGU Advances, 2, e2020AV000208. https://doi.org/10.1029/2020AV000208
Bralower, T. J., Cosmidis, J., Heaney, P. J., Kump, L. R., Morgan, J. V., Harper, D. T., et al. (2020). Origin of a global carbonate layer deposited in the aftermath of the Cretaceous-Paleogene boundary impact. Earth and Planetary Science Letters, 548, 116476. https://doi.org/10.1016/j.epsl.2020.116476
Bralower, T. J., Silva, I. P., Malone, M. J., & Scientific Participants of Leg 198, fnm (2002). New evidence for abrupt climate change in the Cretaceous and Paleogene: An ocean drilling program expedition to Shatsky Rise, northwest Pacific. Geological Society of America Today, 12, 4–10. https://doi.org/10.1130/1052-5173(2002)012<0004:nefacc>2.0.co;2
Brugger, J., Feulner, G., Hofmann, M., & Petri, S. (2021). A pronounced spike in ocean productivity triggered by the Chicxulub impact. Geophysical Research Letters, e2020GL092260. https://doi.org/10.1029/2020gl092260
Brugger, J., Feulner, G., & Petri, S. (2017). Baby, it's cold outside: Climate model simulations of the effects of the asteroid impact at the end of the Cretaceous. Geophysical Research Letters, 44, 419–427. https://doi.org/10.1002/2016gl072241
Buessler, K. O. (1998). The decoupling of production and particulate export in the surface ocean. Global Biogeochemical Cycles, 12(2), 297–310.

Buesseler, K. O., & Boyd, P. W. (2009). Shedding light on processes that control particle export and flux attenuation in the twilight zone of the open ocean. Limnology and Oceanography, 54(4), 1210–1232. https://doi.org/10.4319/lo.2009.54.4.1210
Coccioni, R., Frontalini, F., Bancalà, G., Fornaciari, E., Jovane, L., & Sprovieri, M. (2010). The Dan-C2 hyperthermal event at Gubbio (Italy): Global implications, environmental effects, and cause(s). Earth and Planetary Science Letters, 297, 298–305. https://doi.org/10.1016/j.epsl.2010.06.031
Coxall, H. K., D'Hondt, S., & Zachos, J. C. (2006). Pelagic evolution and environmental recovery after the Cretaceous-Paleogene mass extinction. Geology, 34(4), 297–300. https://doi.org/10.1130/g21702.1
Culver, S. J. (1988). New foraminiferal depth zonation of the northwestern Gulf of Mexico. Palaios, 3, 69–85. https://doi.org/10.2307/3514545
Culver, S. J., & Buzas, M. A. (2000). Global latitudinal species diversity gradient in deep-sea benthic foraminifera. Deep Sea Research Part I: Oceanographic Research Papers, 47(2), 259–275. https://doi.org/10.1016/s0967-0637(99)00055-2
De La Rocha, C. L., & Passow, U. (2007). Factors influencing the sinking of POC and the efficiency of the biological carbon pump. Deep Sea Research Part II: Topical Studies in Oceanography, 54(5–7), 639–658. https://doi.org/10.1016/j.dsr2.2007.01.004
D'Hondt, S., Donaghay, P., Zachos, J. C., Luttenberg, D., & Lindinger, M. (1998). Organic carbon fluxes and ecological recovery from the Cretaceous-Tertiary mass extinction. Science, 282, 276–279. https://doi.org/10.1126/science.282.5387.276
D'Hondt, S., & Keller, G. (1991). Some patterns of planktic foraminiferal assemblage turnover at the Cretaceous-Tertiary boundary. Marine Micropaleontology, 17, 77–118. https://doi.org/10.1016/0377-8398(91)90024-z
D'Hondt, S., & Zachos, J. C. (1993). On stable isotopic variation and earliest Paleocene planktonic foraminifera. Paleoceanography, 8, 527–547. https://doi.org/10.1029/93pa00952
D'Onofrio, R., Luciani, V., Fornaciari, E., Giusberti, L., Boscolo Galazzo, F., Dallanave, E., et al. (2016). Environmental perturbations at the early Eocene ETM2, H2, and I1 events as inferred by Tethyan calcareous plankton (Terche section, northeastern Italy). Paleoceanography, 31(9), 1225–1247. https://doi.org/10.1002/2016pa002940
Dymond, J., Suess, E., & Lyle, M. (1992). Barium in deep-sea sediment: A geochemical proxy for paleoproductivity. Paleoceanography, 7, 163–181. https://doi.org/10.1029/92PA00181
Eagle, M., Paytan, A., Arrigo, K. R., van Dijken, G., & Murray, R. W. (2003). A comparison between excess barium and barite as indicators of carbon export. Paleoceanography, 18, 1021. https://doi.org/10.1029/2002PA000793
Edgar, K. M., Wilson, P. A., Sexton, P. F., & Suganuma, Y. (2007). No extreme glaciation during the main Eocene calcite compensation depth shift. Nature, 448, 908–911. https://doi.org/10.1038/nature06053
Fraass, A. J., Kelly, D. C., & Peters, S. E. (2015). Macroevolutionary history of the planktic foraminifera. Annual Review of Earth and Planetary Sciences, 43, 139–166. https://doi.org/10.1146/annurev-earth-060614-105059
Francois, R., Honjo, S., Manganini, S. J., & Ravizza, G. E. (1995). Biogenic barium fluxes to the deep sea: Implications for paleoproductivity reconstruction. Global Biogeochemical Cycles, 9, 289–303. https://doi.org/10.1029/95GB00021
Galloway, W. E., Ganey-Curry, P. E., Li, X., & Buffler, R. T. (2000). Cenozoic depositional history of the Gulf of Mexico basin. AAPG Bulletin, 84, 1743–1774. https://doi.org/10.1306/8626c37f-173b-11d7-8645000102c1865d
Gibbs, S. J., Bown, P. R., Ward, B. A., Alvarez, S. A., Kim, H., Archontikis, O. A., et al. (2020). Algal plankton turn to hunting to survive and recover from end-Cretaceous impact darkness. Science Advances, 6(44), eabc9123. https://doi.org/10.1126/sciadv.abc9123
Gibbs, S. J., Bralower, T. J., Bown, P. R., Zachos, J. C., & Bybell, L. M. (2006). Shelf and open-ocean calcareous phytoplankton assemblages across the Paleocene-Eocene thermal maximum: Implications for global productivity gradients. Geology, 34, 233–236. https://doi.org/10.1130/g22381.1
Gooday, A. J. (2003). Benthic Foraminifera (Protista) as tools in deep-water palaeoceanography: Environmental influences on faunal characteristics. Advances in Marine Biology, 46, 1–90. https://doi.org/10.1016/s0065-2881(03)46002-1
Govin, A., Holzwarth, U., Heslop, D., Ford Keeling, L., Zabel, M., Mulitza, S., et al. (2012). Distribution of major elements in Atlantic surface sediments (36°N–49°S): Imprint of terrigenous input and continental weathering. Geochemistry, Geophysics, Geosystems, 13. https://doi.org/10.1029/2011gc003785
Gradstein, F. M., Ogg, J. G., Schmitz, M., & Ogg, G. (Eds.). (2012). The geologic times scale 2012. Elsevier B.V.
Griffith, E. M., & Paytan, A. (2012). Barite in the ocean–occurrence, geochemistry and palaeoceanographic applications. Sedimentology, 59, 1817–1835. https://doi.org/10.1111/j.1365-3091.2012.01327.x
Griffith, E. M., Thomas, E., Lewis, A. R., Penman, D. E., Westerhold, T., & Winguth, A. M. (2021). Bentho-Pelagic decoupling: The marine biological carbon pump during Eocene hyperthermals. Paleoceanography and Paleoclimatology, 36(3), e2020PA004053. https://doi.org/10.1029/2020pa004053
Gulick, S., Morgan, J., Mellett, C. L., Green, S. L., Bralower, T., Chenot, E., et al. (2017). Site M0077: Post-impact sedimentary rocks. In J. Morgan, S. Gulick, C. L. Mellett, S. L. Green, & the Expedition 364 scientists (Eds.), Chicxulub: Drilling the K-Pg impact crater. Proceedings of the International Ocean Discovery Program, 364: College Station, TX (International Ocean Discovery Program). https://doi.org/10.14379/iodp.proc.364.105.2017
Gulick, S. P., Barton, P. J., Christeson, G. L., Morgan, J. V., McDonald, M., Mendoza-Cervantes, K., et al. (2008). Importance of pre-impact crustal structure for the asymmetry of the Chicxulub impact crater. Nature Geoscience, 1, 131–135. https://doi.org/10.1038/ngeo103
Gulick, S. P. S., Bralower, T. J., Ormö, J., Hall, B., Grice, K., Schaefer, B., et al. (2019). The first day of the Cenozoic. Proceedings of the National Academy of Sciences, 116, 19342–19351. https://doi.org/10.1073/pnas.1909479116
Hemleben, C., Mühlen, D., Olsson, R. K., & Berggren, W. A. (1991). Surface texture and the first occurrence of spines in planktonic foraminifera from the early Tertiary. Geologisches Jahrbuch, 128, 117–146.
Henehan, M. J., Ridgwell, A., Thomas, E., Zhang, S., Alegret, L., Schmidt, D. N., et al. (2019). Rapid ocean acidification and protracted Earth system recovery followed the end-Cretaceous Chicxulub impact. Proceedings of the National Academy of Sciences, 116(45), 22500–22504. https://doi.org/10.1073/pnas.1905989116
Henson, S. A., Sanders, R., & Madsen, E. (2012). Global patterns in efficiency of particulate organic carbon export and transfer to the deep ocean. Global Biogeochemical Cycles, 26, GB1028. https://doi.org/10.1029/2011GB004099
Herguera, J. C., & Berger, W. (1991). Paleoproductivity from benthic foraminifera abundance: Glacial to postglacial change in the west-equatorial Pacific. Geology, 19(12), 1173–1176. https://doi.org/10.1130/0091-7613(1991)019<1173:pfbfag>2.3.co;2
Hildebrand, A. R., Penfield, G. T., Kring, D. A., Pilkington, M., Camargo, A. Z., Jacobsen, S. B., & Boynton, W. V. (1991). Chicxulub crater: A possible Cretaceous/Tertiary boundary impact crater on the Yucatán Peninsula. Mexico Geology, 19, 867–871. https://doi.org/10.1130/0091-7613(1991)019<0867:ccapct>2.3.co;2
Hilting, A. K., Kump, L. R., & Bralower, T. J. (2008). Variations in the oceanic vertical carbon isotope gradient and their implications for the Paleocene-Eocene biological pump. Paleoceanography, 23(3), PA3222. https://doi.org/10.1029/2007pa001458

Hsü, K. J., & McKenzie, J. A. (1985). A "strangelove" ocean in the earliest tertiary. The carbon cycle and atmospheric CO: Natural variations Archean to present. (pp. 487–492).
Hull, P. M., et al. (2020). On impact and volcanism across the Cretaceous-Paleogene boundary. Science, 367(6475), 266–272. https://doi.org/10.1126/science.aay5055
Hull, P. M., & Norris, R. D. (2011). Diverse patterns of ocean export productivity change across the Cretaceous-Paleogene boundary: New insights from biogenic barium. Paleoceanography, 26(3), PA3205. https://doi.org/10.1029/2010pa002082
Hull, P. M., Norris, R. D., Bralower, T. J., & Schueth, J. D. (2011). A role for chance in marine recovery from the end-Cretaceous extinction. Nature Geoscience, 4, 856–860. https://doi.org/10.1038/ngeo1302
Jablonski, D. (1995). In J. H. Lawton, & R. M. May (Eds.), (Eds), *Extinction rates*. Oxford University Press.
Jones, H., Lowery, C. M., & Bralower, T. (2019). Delayed calcareous nannoplankton boom-bust successions in the earliest Paleocene Chicxulub (Mexico) impact crater. Geology, 47, 753–756. https://doi.org/10.1130/G46143.1
Jorissen, F. J., de Stigter, H. C., & Widmark, J. G. V. (1995). A conceptual model explaining benthic foraminiferal microhabitats. Marine Micropaleontology, 26, 3–15. https://doi.org/10.1016/0377-8398(95)00047-x
Kaiho, K., Oshima, N., Adachi, K., Adachi, Y., Mizukami, T., Fujibayashi, M., & Saito, R. (2016). Global climate change driven by soot at the K-Pg boundary as the cause of the mass extinction. Scientific Reports, 6(1), 1–13. https://doi.org/10.1038/srep28427
Keller, G. (1989). Extended Cretaceous/Tertiary boundary extinctions and delayed population change in planktonic foraminifera from Brazos River, Texas. Paleoceanography and Paleoclimatology, 4, 287–332. https://doi.org/10.1029/pa004i003p00287
Kring, D. A. (2007). The Chicxulub impact event and its environmental consequences at the Cretaceous–Tertiary boundary. Palaeogeography, Palaeoclimatology, Palaeoecology, 255, 4–21. https://doi.org/10.1016/j.palaeo.2007.02.037
Kring, D. A., Tikoo, S. M., Schmieder, M., Riller, U., Rebolledo-Vieyra, M., Simpson, S. L., (2020). Probing the hydrothermal system of the Chicxulub impact crater. Science Advances, 6(22). eaaz3053. https://doi.org/10.1126/sciadv.aaz3053
Lam, P. J., Doney, S. C., & Bishop, J. K. B. (2011). The dynamic ocean biological pump: Insights from a global compilation of particulate organic carbon, $CaCO_3$ and opal concentration profiles from the mesopelagic. Global Biogeochemical Cycles, 27, GB3009. https://doi.org/10.1029/2010gb003868
Leckie, R. M., Bralower, T. J., & Cashman, R. (2002). Oceanic anoxic events and plankton evolution: Biotic response to tectonic forcing during the mid-Cretaceous. Paleoceanography, 17, 13–21. https://doi.org/10.1029/2001pa000623
Leckie, R. M., & Olson, H. C. (2003). Foraminifera as proxies for sea-level change on siliciclastic margins. In H. C. Olson, & R. M. Leckie (Eds.), Micropaleontologic proxies for sea-level change and stratigraphic discontinuities (pp. 5–19). SEPM Special Publication No 75. https://doi.org/10.2110/pec.03.75.0005
Legendre, L., & Rivkin, R. B. (2002). Fluxes of carbon in the upper ocean: Regulation by food-web control nodes. Marine Ecology Progress Series, 242, 95–109. https://doi.org/10.3354/meps242095
Liebrand, D., Raffi, I., Fraguas, Á., Laxenaire, R., Bosmans, J. H., Hilgen, F. J., et al. (2018). Orbitally forced hyperstratification of the Oligocene South Atlantic Ocean. Paleoceanography and paleoclimatology, 33(5), 511–529. https://doi.org/10.1002/2017pa003222
Lirer, F. (2000). A new technique for retrieving calcareous microfossils from lithified lime deposits. Micropaleontology, 46, 365–369.
Liu, C., & Olsson, R. K. (1992). Evolutionary radiation of microperforate planktonic foraminifera following the K/T mass extinction event. Journal of Foraminiferal Research, 22, 328–346. https://doi.org/10.2113/gsjfr.22.4.328
Liu, Q., Roberts, A. P., Larrasoana, J. C., Banerjee, S. K., Guyodo, Y., Tauxe, L., & Oldfield, F. (2012). Environmental magnetism: Principles and applications. Reviews of Geophysics, 50, RG4002. https://doi.org/10.1029/2012RG000393
Lowery, C. M., Bown, P. R., Fraass, A. J., & Hull, P. M. (2020). Ecological response of plankton to environmental change: Thresholds for extinction. Annual Review of Earth and Planetary Sciences, 48, 403–429. https://doi.org/10.1146/annurev-earth-081619-052818
Lowery, C. M., Bralower, T. J., Owens, J. D., Rodríguez-Tovar, F. J., Jones, H., Smit, J., et al. (2018). Rapid recovery of life at ground zero of the end Cretaceous mass extinction. Nature, 558, 288–291. https://doi.org/10.1038/s41586-018-0163-6
Lyons, S. L., Karp, A. T., Bralower, T. J., Grice, K., Schaefer, B., Gulick, S. P., et al. (2020). Organic matter from the Chicxulub crater exacerbated the K–Pg impact winter. Proceedings of the National Academy of Sciences, 117(41), 25327–25334. https://doi.org/10.1073/pnas.2004596117
Marsay, C. M., Sanders, R. J., Henson, S. A., Pabortsava, K., Achterberg, E. P., & Lampitt, R. S. (2015). Attenuation of sinking particulate organic carbon flux through the mesopelagic ocean. Proceedings of the National Academy of Sciences, 112(4), 1089–1094. https://doi.org/10.1073/pnas.1415311112
Miller, K. G., Browning, J. V., Schmelz, W. J., Kopp, R. E., Mountain, G. S., & Wright, J. D. (2020). Cenozoic sea-level and cryospheric evolution from deep-sea geochemical and continental margin records. Science Advances, 6(20), eaaz1346. https://doi.org/10.1126/sciadv.aaz1346
Minoletti, F., De Rafélis, M., Renard, M., Gardin, S., & Young, J. (2005). Changes in the pelagic fine fraction carbonate sedimentation during the Cretaceous–Paleocene transition: Contribution of the separation technique to the study of Bidart section. Palaeogeography, Palaeoclimatology, Palaeoecology, 216(1–2), 119–137. https://doi.org/10.1016/j.palaeo.2004.10.006
Morgan, J. V., Gulick, S. P. S., Mellet, C. L., Green, S. L., & Expedition 364 Scientists (2017). *Chicxulub: Drilling the K-Pg Impact Crater, Proceedings of the International Ocean Discovery Program, 364*, International Ocean Discovery Program, College Station, TX. https://doi.org/10.14379/iodp.proc.364.103.2017
Murray, J. W. (1976). A method of determining proximity of marginal seas to an ocean. Marine Geology, 22, 103–119. https://doi.org/10.1016/0025-3227(76)90033-5
Norris, R. D. (1996). Symbiosis as an evolutionary innovation in the radiation of Paleocene planktic foraminifera. Paleobiology, 22, 461–480. https://doi.org/10.1017/s0094837300016468
Okada, H., & Bukry, D. (1980). Supplementary modification and introduction of code numbers to the low-latitude coccolith biostratigraphic zonation (Bukry, 1973; 1975). Marine Micropaleontology, 5, 321–325. https://doi.org/10.1016/0377-8398(80)90016-x
Olsson, R. K., Berggren, W. A., Hemleben, C. I., & Huber, B. T. (1999). Atlas of Paleocene planktonic foraminifera. *Smithsonian Contributions to Paleobiology* 85. https://doi.org/10.5479/si.00810266.85.1
Paytan, A., & Griffith, E. M. (2007). Marine barite: Recorder of variations in ocean export productivity. In V. Gornitz (Ed.), Encyclopedia of paleoclimate and ancient environments (pp. 643–651). Springer. https://doi.org/10.1016/j.dsr2.2007.01.007
Paytan, A., Kastner, M., & Chavez, F. P. (1996). Glacial to interglacial fluctuations in productivity in the equatorial Pacific as indicated by marine barite. Science, 274, 1355–1357. https://doi.org/10.1126/science.274.5291.1355
Pearson, P. N., Olsson, R. K., Huber, B. T., Hemleben, C., & Berggren, W. A. (2006). Atlas of Eocene planktonic foraminifera (Vol. 41). Cushman Foundation for Foraminiferal Research Special Publications 513.

Pearson, P. N., Shackleton, N. J., & Hall, M. A. (1993). Stable isotope paleoecology of middle Eocene planktonic foraminifera and multi-species isotope stratigraphy, DSDP Site 523, South Atlantic. Journal of Foraminiferal Research, 23(2), 123–140. https://doi.org/10.2113/gsjfr.23.2.123

Perch-Nielsen, K. (1985). Cenozoic calcareous nannofossils. In H. M. Bolli, J. B. Saunders, & K. Perch-Nielsen (Eds.), Plankton stratigraphy (pp. 427–554). Cambridge University Press.

Pope, K. O., Baines, K. H., Ocampo, A. C., & Ivanov, B. A. (1994). Impact winter and the Cretaceous/Tertiary extinctions: Results of a Chicxulub asteroid impact model. Earth and Planetary Science Letters, 128(3–4), 719–725. https://doi.org/10.1016/0012-821x(94)90186-4

Quillévéré, F., Norris, R. D., Kroon, D., & Wilson, P. A. (2008). Transient ocean warming and shifts in carbon reservoirs during the early Danian. Earth and Planetary Science Letters, 265, 600–615. https://doi.org/10.1016/j.epsl.2007.10.040

Rodriguez-Tovar, F. J., Lowery, C. M., Bralower, T. J., Gulick, S. P. S., & Jones, H. L. (2020). Rapid microbenthic diversification and stabilization after the end-Cretaceous mass extinction event. Geology, 48, 1048–1052. https://doi.org/10.1130/g47589.1

Rothwell, R., & Croudace, I. (2015). Twenty years of XRF core scanning marine sediments: What do geochemical proxies tell us? In I. Croudace, & R. Rothwell (Eds.), Micro-XRF Studies of sediment cores. Developments in paleoenvironmental research, 17. Springer.

Schaefer, B., Grice, K., Coolen, M. J. L., Summons, R. E., Cui, X., Bauersachs, T., et al. (2020). Microbial life in the nascent Chicxulub crater. Geology, 48, 328–332. https://doi.org/10.1130/G46799.1

Schulte, P., Alegret, L., Arenillas, I., Arz, J. A., Barton, P. J., Bown, P. R., et al. (2010). The Chicxulub asteroid impact and mass extinction at the Cretaceous-Paleogene boundary. Science, 327, 1214–1218. https://doi.org/10.1126/science.1177265

Sepúlveda, J., Alegret, L., Thomas, E., Haddad, E., Cao, C., & Summons, R. E. (2019). Stable isotope constraints on marine productivity across the Cretaceous-Paleogene mass extinction. Paleoceanography and Paleoclimatology, 34(7), 1195–1217. https://doi.org/10.1029/2018pa003442

Sepúlveda, J., Wendler, J. E., Summons, R. E., & Hinrichs, K. U. (2009). Rapid resurgence of marine productivity after the Cretaceous-Paleogene mass extinction. Science, 326, 129–132. https://doi.org/10.1126/science.1176233

Smit, J., & Hertogen, J. (1980). An extraterrestrial event at the Cretaceous-Tertiary boundary. Nature, 285, 198–200. https://doi.org/10.1038/285198a0

Smith, V., Warny, S., Grice, K., Schaefer, B., Whalen, M. T., Vellekoop, J., et al. (2020). Life and death in the Chicxulub impact crater: A record of the Paleocene-Eocene thermal maximum (PETM). Climate of the Past, 16, 1889–1899. https://doi.org/10.5194/cp-16-1889-2020

Tabor, C. R., Bardeen, C. G., Otto-Bliesner, B. L., Garcia, R. R., & Toon, O. B. (2020). Causes and climatic consequences of the impact winter at the Cretaceous-Paleogene boundary. Geophysical Research Letters, 47, e60121. https://doi.org/10.1029/2019gl085572

Thunell, R. C. (1976). Optimum indices of calcium carbonate dissolution, in deep-sea sediments. Geology, 4, 525–528. https://doi.org/10.1130/0091-7613(1976)4<525:oioccd>2.0.co;2

Troelsen, J. C. (1957). Some planktonic foraminifera of the type Danian and their stratigraphic importance. U S National Museum Bulletin, 215, 125–131.

Tschudy, R. H., Pillmore, C. L., Orth, C. J., Gilmore, J. S., & Knight, J. D. (1984). Disruption of the terrestrial plant ecosystem at the Cretaceous-Tertiary boundary, Western Interior. Science, 225(4666), 1030–1032. https://doi.org/10.1126/science.225.4666.1030

Tsikos, H., Jenkyns, H. C., Walsworth-Bell, B., Petrizzo, M. R., Forster, A., Kolonic, S., et al. (2004). Carbon-isotope stratigraphy recorded by the Cenomanian–Turonian Oceanic Anoxic Event: Correlation and implications based on three key localities. Journal of the Geological Society, 161(4), 711–719. https://doi.org/10.1144/0016-764903-077

Vajda, V., Raine, J. I., Hollis, C. J., & Strong, C. P. (2004). Global effects of the Chicxulub impact on terrestrial vegetation—Review of the palynological record from New Zealand Cretaceous/Tertiary boundary. In Cratering in marine environments and on ice (pp. 57–74). Springer. https://doi.org/10.1007/978-3-662-06423-8_4

Van der Zwaan, G. J., Jorissen, F. J., & Stitger, H. C. (1990). The depth dependency of planktonic/benthic foraminiferal ratios: Constraints and applications. Marine Geology, 95, 1–16. https://doi.org/10.1016/0025-3227(90)90016-d

Van Hinsbergen, D. J. J., Kouwenhoven, T. J., & Van der Zwaan, G. J. (2005). Paleobathymetry in the backstripping procedure: Correction of oxygenation effects on depth estimates. Palaeogeography, Palaeoclimatology, Palaeoecology, 21, 245–265. https://doi.org/10.1016/j.palaeo.2005.02.013

Vellekoop, J., Esmeray-Senlet, S., Miller, K. G., Browning, J. V., Sluijs, A., van de Schootbrugge, B., et al. (2016). Evidence for Cretaceous-Paleogene boundary bolide "impact winter" conditions from New Jersey, USA. Geology, 44(8), 619–622. https://doi.org/10.1130/g37961.1

Vellekoop, J., Sluijs, A., Smit, J., Schouten, S., Weijers, J. W. H., Sinninghe Damsté, J. S., & Brinkhuis, H. (2014). Rapid short-term cooling following the Chicxulub impact at the Cretaceous–Paleogene boundary. Proceedings of the National Academy of Sciences, 111, 7537–7541. https://doi.org/10.1073/pnas.1319253111

Vellekoop, J., Woelders, L., Açikalin, S., Smit, J., Van De Schootbrugge, B., Yilmaz, I. O., et al. (2017). Ecological response to collapse of the biological pump following the mass extinction at the Cretaceous-Paleogene boundary. Biogeosciences, 14, 885–900. https://doi.org/10.5194/bg-14-885-2017

Wade, B. S., Pearson, P. N., Berggren, W. A., & Pälike, H. (2011). Review and revision of Cenozoic tropical planktonic foraminiferal biostratigraphy and calibration to the geomagnetic polarity and astronomical time scale. Earth-Science Reviews, 104, 111–142. https://doi.org/10.1016/j.earscirev.2010.09.003

Weber, T., Cram, J. A., Leung, S. W., DeVries, T., & Deutsch, C. (2016). Deep ocean nutrients imply large latitudinal variation in particle transfer efficiency. Proceedings of the National Academy of Sciences, 113(31), 8606–8611. https://doi.org/10.1073/pnas.1604414113

Wolbach, W. S., Lewis, R. S., & Anders, E. (1985). Cretaceous extinctions: Evidence for wildfires and search for meteoritic material. Science, 230(4722), 167–170.

Zachos, J. C., Arthur, M. A., & Dean, W. E. (1989). Geochemical evidence for suppression of pelagic marine productivity at the Cretaceous/Tertiary boundary. Nature, 337, 61–64. https://doi.org/10.1038/337061a0

Zhang, C., Dang, H., Azam, F., Benner, R., Legendre, L., Passow, U., et al. (2018). Evolving paradigms in biological carbon cycling in the ocean. National Science Review, 5, 481–499. https://doi.org/10.1093/nsr/nwy074

Ziegler, M., Lourens, L. J., Tuenter, E., & Reichart, G. J. (2009). Anomalously high Arabian Sea productivity conditions during MIS 13. Climate of the Past Discussions, 5, 1989–2018. https://doi.org/10.5194/cp-6-63-2010